ELSEVIER

Journal of Chemical Neuroanatomy 13 (1997) 219–241

Journal of Chemical Neuroanatomy

Differential plasma membrane distribution of metabotropic glutamate receptors mGluR1α, mGluR2 and mGluR5, relative to neurotransmitter release sites

Rafael Luján [a,*], J. David B. Roberts [a], Ryuichi Shigemoto [b], Hitoshi Ohishi [b], Peter Somogyi [a]

[a] *Medical Research Council, Anatomical Neuropharmacology Unit, Department of Pharmacology, Oxford University, Mansfield Road, Oxford OX1 3TH, UK*

[b] *Department of Morphological Brain Science, Faculty of Medicine, Kyoto University, Sakyo-ku, Kyoto 606, Japan*

Received 1 May 1997; accepted 21 June 1997

Abstract

Two group I metabotropic glutamate receptor subtypes, mGluR1 and mGluR5, have been reported to occur in highest concentration in an annulus surrounding the edge of the postsynaptic membrane specialisation. In order to determine whether such a distribution is uniform amongst postsynaptic mGluRs, their distribution was compared quantitatively by a pre-embedding silver-intensified immunogold technique at electron microscopic level in hippocampal pyramidal cells (mGluR5), cerebellar Purkinje cells (mGluR1α) and Golgi cells (mGluR2). The results show that mGluR1α, mGluR5 and mGluR2 each have a distinct distribution in relation to the glutamatergic synaptic junctions. On dendritic spines, mGluR1α and mGluR5 showed the highest receptor density in a perisynaptic annulus (defined as within 60 nm of the edge of the synapse) followed by a decreasing extrasynaptic (60–900 nm) receptor level, but the gradient of decrease and the proportion of the perisynaptic pool (mGluR1α, ~50%; vs mGluR5, ~25%) were different for the two receptors. The distributions of mGluR1α and mGluR5 also differed significantly from simulated random distributions. In contrast, mGluR2 was not closely associated with glutamatergic synapses in the dendritic plasma membrane of cerebellar Golgi cells and its distribution relative to synapses is not different from simulated random distribution in the membrane. The somatic membrane, the axon and the synaptic boutons of the GABAergic Golgi cells also contained immunoreactive mGluR2 that is not associated with synaptic specialisations. In the hippocampal CA1 area the distribution of immunoparticles for mGluR5 on individual spines was established using serial sections. The results indicate that dendritic spines of pyramidal cells are heterogeneous with respect to the ratio of perisynaptic to extrasynaptic mGluR5 pools and about half of the immunopositive spines lack the perisynaptic pool. The quantitative comparison of receptor distributions demonstrates that mGluR1α and mGluR5, but not mGluR2, are highly compartmentalised in different plasma membrane domains. The unique distribution of each mGluR subtype may reflect requirements for different transduction and effector mechanisms between cell types and different domains of the same cell, and suggests that the precise placement of receptors is a crucial factor contributing to neuronal communication. © 1997 Elsevier Science B.V.

Keywords: Hippocampus; Cerebellum; Immunocytochemistry; Glutamate; Synaptic junction; Quantitative immunogold

1. Introduction

The response to synaptically released glutamate is mediated by activation of multiple excitatory amino acid receptors in the brain, including those which form ion channels (ionotropic) and those (metabotropic)

* Corresponding author. Tel.: +44 1865 271604; fax: +44 1865 271648.

PII S0891-0618(97)00051-3

which are coupled via G-proteins and second messengers to various effector mechanisms (Eaton et al., 1993; Miles and Poncer, 1993; Seeburg, 1993; Batchelor et al., 1994; Hollmann and Heinemann, 1994; Nakanishi, 1994; Masu et al., 1995). The two classes of excitatory amino acid receptors interact in the fine-tuning of neuronal responses under different conditions. Activation of mGluRs leads to a variety of physiological responses (Eaton et al., 1993; Hayashi et al., 1993; Gereau and Conn, 1995; Guerineau et al., 1995; Masu et al., 1995; Yokoi et al., 1996) depending on the mGluR subtype, the transduction and effector mechanisms and the receptor distribution in relation to neurotransmitter release sites.

Eight metabotropic glutamate receptors (mGluR1–8) have been cloned (Nakanishi, 1994; Duvoisin et al., 1995), several of which exist in alternately spliced variants. These mGluRs are grouped according to the degree of sequence homology, transduction mechanisms and agonist selectivity. Group I includes mGluR1 and mGluR5, which stimulate phosphatidylinositol hydrolysis and intracellular Ca^{2+} release and are activated by quisqualate as their most potent agonist (Masu et al., 1991; Abe et al., 1992; Aramori and Nakanishi, 1992). Group II is composed of mGluR2 and mGluR3, which are coupled to an inhibitory cascade of cyclic AMP (cAMP) formation in heterologous expression systems and are most potently activated by 2*R*,4*R*-4-aminopyrrolidine-2,4-dicarboxylate (APDC; Tanabe et al., 1992, 1993; Schoepp et al., 1995). The others, mGluR4, 6, 7 and 8 comprise group III, they also inhibit cAMP formation in expression systems and are potently activated by L-amino-4-phosphonobutyrate (L-AP4; Tanabe et al., 1992; Nakajima et al., 1993; Tanabe et al., 1993; Okamoto et al., 1994; Duvoisin et al., 1995).

In the rat brain, the activation of mGluRs contributes to both postsynaptic and presynaptic responses (Miles and Poncer, 1993; Gereau and Conn, 1995; Poncer et al., 1995; Sánchez-Prieto et al., 1996). Immunocytochemical studies have established that mGluR1 and 5 are exclusively postsynaptic in the hippocampus (Martin et al., 1992; Shigemoto et al., 1993; Lujan et al., 1996, but see Romano et al., 1995). In contrast, mGluR2/3 are present at both presynaptic and postsynaptic sites in cerebellar Golgi cells (Ohishi et al., 1994; Neki et al., 1996a,b), and in the olfactory bulb (Hayashi et al., 1993), but in the hippocampus are mainly found presynaptically (Shigemoto et al., 1995; Petralia et al., 1996). Group III mGluRs have been found mainly (Bradley et al., 1996), or exclusively presynaptically in the hippocampus (Shigemoto et al., 1996) and spinal cord (Ohishi et al., 1995), and both pre- and post-synaptically in the retina (Brandstatter et al., 1996).

The precise location and density of glutamate receptors on the cell surface may be a critical factor for specifying signalling within and between neurons. Restricted location to one cellular compartment may indicate a single functional role, whereas the presence of a receptor in functionally distinct domains of neurons may indicate multiple roles. Group I and II mGluRs, the subject of the present study, can be present in different concentration in distinct cellular domains on the same neuron. For example mGluR1 and 5 were found to be highly concentrated on dendritic spines, but they were also present at a lower density in the somato-dendritic membrane of hippocampal pyramidal cells (Lujan et al., 1996). Likewise, mGluR2/3 were present in both the somato-dendritic and axonal domains of cerebellar GABAergic Golgi cells (Ohishi et al., 1994; Neki et al., 1996a,b). In addition, in all the cell types studied to date, group I mGluRs were found to be concentrated in an annulus surrounding the edge of glutamatergic postsynaptic membrane specialisations (Baude et al., 1993; Nusser et al., 1994; Lujan et al., 1996). Quantitative studies carried out for mGluR5 have indicated that at least 25% of receptor in dendritic spines is located at the immediate edge of the membrane specialisation (Lujan et al., 1996). In order to determine whether such a distribution is uniform amongst postsynaptic mGluRs, their distribution was compared quantitatively by a pre-embedding silver-intensified immunogold technique at electron microscopic level in hippocampal pyramidal cells (mGluR5), cerebellar Purkinje cells (mGluR1α) and Golgi cells (mGluR2). Moreover, the possibility that hippocampal CA1 pyramidal cell spines immunoreactive for mGluR5 may be heterogeneous with regard to the precise location of receptors was also investigated on dendritic spines using serial sections.

2. Material and methods

Eight adult female Wistar rats (200–250 g) were deeply anaesthetised with Sagatal (pentobarbitone sodium, 60 mg/ml i.p.) and perfused through the ascending aorta for 13–18 min, first with 0.9% saline for 1 min followed by freshly prepared ice-cold fixative containing 4% paraformaldehyde, either 0.025 or 0.05% glutaraldehyde and $\sim$0.2% picric acid made up in 0.1 M phosphate buffer (PB; pH $\sim$ 7.4). Immunoreactivity could be detected using both fixatives, but labelling was weaker using the higher concentration of glutaraldehyde. After perfusion, brains were removed from the skull and blocks of tissue containing the hippocampus and cerebellum were dissected and washed in 0.1 M PB for several hours.

2.1. Antibodies

The three mGluRs were visualised by affinity-purified rabbit (mGluR1α and mGluR5) or guinea pig

(mGluR2/3) polyclonal antibodies and a monoclonal antibody to mGluR2. The production and characterisation of the anti-mGluR1α (Baude et al., 1993), anti-mGluR5 (Shigemoto et al., 1993) and monoclonal anti-mGluR2 antibodies have been described elsewhere. Briefly, antibodies to mGluR1α (code no. A4) were raised to a synthetic peptide derived from the C-terminal, cytoplasmic region (residues 1117–1130) of the receptor. The antibodies reacted with a 160 kDa band in Western blots and specificity was also confirmed on expressed receptors (Baude et al., 1993). Antibodies to mGluR5 (code no. G53) were raised against a fusion protein containing the C-terminal amino acid sequence (residues 863–1171) of the intracellular domain (Abe et al., 1992), which is present in both the mGluR5a and mGluR5b splice variants (Minakami et al., 1993). In immunoblot analysis of crude membrane preparations from rat brain, a major band with an estimated molecular weight of 145 kDa was detected and the specificity of the antibodies was also confirmed on cDNA-transfected COS cells (Shigemoto et al., 1993). The monoclonal antibody (code: mG2Na-5) was raised to a fusion protein containing the amino acid residues 87–134 of mGluR2 (Neki et al., 1996a,b). In Western blots the antibody was shown to label a band with an estimated molecular weight of 102 kDa from brain and bands of 97 and 111 kDa were detected from COS cells transfected with cDNA encoding mGluR2. No immunoreactivity was detected in COS cells transfected with cDNA encoding mGluR3 (Neki et al., 1996a,b), indicating that the antibody reacts specifically with mGluR2. The immunostaining of fixed brain sections was also in agreement with the specificity of the antibody to mGluR2 (Neki et al., 1996a,b).

Antibodies (code no. MG2C2-GP4) against a synthetic peptide corresponding to a C-terminal sequence of mGluR2 (residues 848–872, Tanabe et al., 1992) were raised in guinea pigs as described previously (Kinoshita et al., 1996). Four guinea pigs were immunised by subcutaneous injection of the peptide conjugated to bovine serum albumin by glutaraldehyde, the animals were boosted after 4 weeks and bled 1–2 weeks after the boost. The collected antisera were purified with sodium sulphate fractionation, followed by affinity chromatography using the C-terminal peptide coupled to a column. For immunoblot analysis, crude membranes prepared from rat cerebellum, and whole brains of wild type and mGluR2-deficient mice (Yokoi et al., 1996), were separated on 7% SDS-PAGE and transferred to PVDF filters (Bio-Rad). The filters were first incubated with the affinity-purified antibodies (0.5 μg/ml) and then with alkaline phosphatase-labeled second antibody (Chemicon) to visualise the reacted bands.

For immunohistochemistry, wild type and mGluR2-deficient mice were anaesthetised and perfused transcardially with a fixative as described previously (Ohishi et al., 1995). Sections for light microscopy were cut at 40 μm thickness and incubated with 0.5 μg/ml affinity-purified antibody in phosphate buffered saline containing 0.1% Triton X-100. They were then incubated with biotinylated second antibody and reacted with an ABC Elite Kit (Vector). The sections were finally reacted with 0.02% diaminobenzidine and 0.003% hydrogen peroxide to visualise peroxidase activity.

The reactivity and specificity of the affinity-purified antibody to mGluR2 was verified by immunoblot using rat, wild type mouse, and mGluR2-deficient mouse brains (Fig. 1). Two major immunoreactive products with estimated molecular weights of 98 and ~200 kDa were observed in the rat cerebellum and wild type mouse brains. These products were weakly detected in heterozygous (+/−) but not in homozygous (−/−) mGluR2-mutant mouse brains, kindly made available by Drs M. Yokoi and S. Nakanishi (Yokoi et al., 1996). All these immunoreactive bands also disappeared in wild type animals by preadsorption of the antibody with the C-terminal peptide. The value of 98 kDa corresponds to the predicted molecular masses of mGluR2 (95 770, Tanabe et al., 1992) and mGluR3 (98 960, Tanabe et al., 1992), which are probably increased by post-translational glycosilation. The higher molecular mass band probably represents an aggregate of receptors (see also Ohishi et al., 1994).

The antibody MG2C2-GP4 was also tested on CHO cell lines (results not illustrated) expressing either mGluR2 or mGluR3 as described earlier (Ohishi et al., 1994). Although the antibodies reacted with mGluR3 expressed in high levels in CHO cell lines as described for a rabbit antibody to mGluR2/3 (code no. H12, Ohishi et al., 1994), crossreactivity of MG2C2-GP4 to mGluR3 seems to be weaker than that of H12. Immunoreactive products corresponding to mGluR3 detected in whole brain with H12 (Ohishi et al., 1994) were much less detected with MG2C2-GP4. Furthermore, labelled bands in immunoblot (Fig. 1A) as well as the immunostaining pattern of the cerebellum (Fig. 1B and C) detected with MG2C2-GP4 were almost totally absent in mGluR2-deficient mice. Although the labelling of mGluR3 in sections where it is present in high concentration cannot be excluded, it is likely that antibodies MG2C2-GP4 mainly recognise mGluR2 in the membrane of rodent cerebellar Golgi cells.

2.2. Immunocytochemistry

Immunocytochemical reactions were carried out as described earlier (Baude et al., 1993; Lujan et al., 1996). The blocks of tissue containing the hippocampus and cerebellum were washed in 0.1 M PB followed by incubation for cryoprotection in 10 and 20% sucrose made up in PB at 4°C overnight. To increase the penetration of the reagents, blocks of tissue were

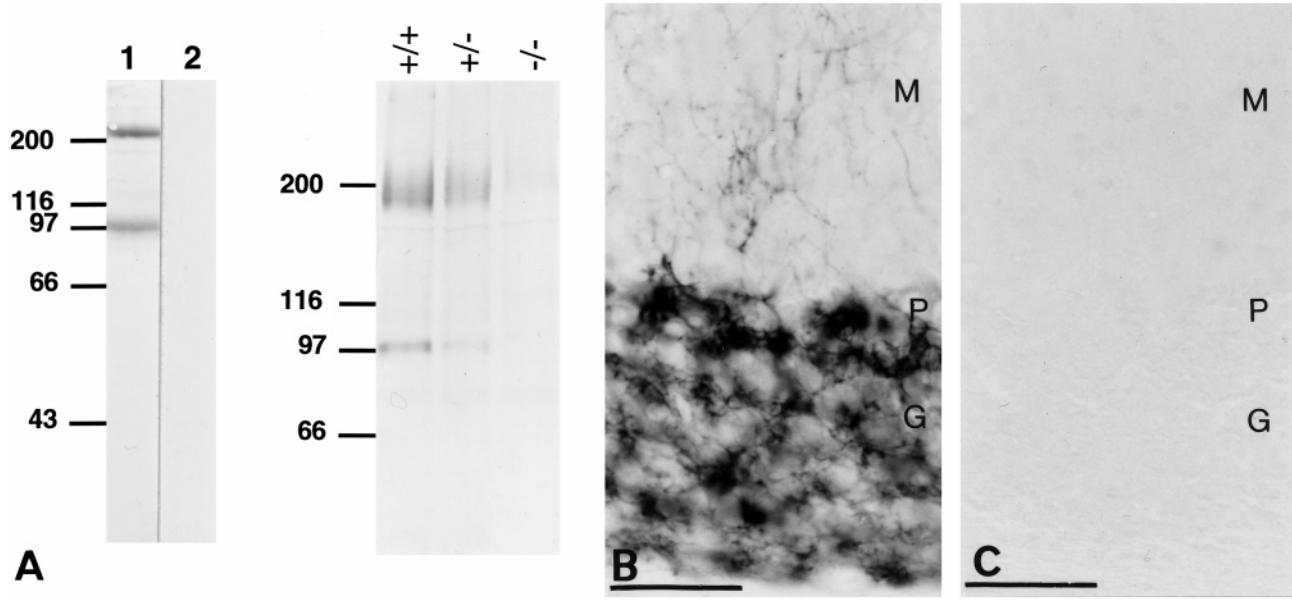

Fig. 1. Characterisation of the affinity-purified antibody MG2C2-GP4 directed to the C-terminal part of rat mGluR2. (A) Immunoblot analysis of the rat cerebellum (lanes 1, 2) and whole mouse brain (+/+, +/− and −/−). Two major bands with estimated molecular weights of 98 and ~200 kDa were detected in rat cerebellum and wild type (+/+) mouse brain. The higher molecular weight bands probably represent an aggregate of receptors. These bands were weakly detected in heterozygous (+/−) mGluR2 mutant mice and completely disappeared in homozygous (−/−) mGluR2 deficient mice. Immunoreactive bands were not detected following preadsorption of the antibody with the peptide (lane 2). (B and C) Immunostaining of wild type (B) and mGluR2 deficient mouse (C) cerebellar cortex. Immunolabelling with antibodies MG2C2-GP4 is present in cerebellar Golgi cells. Golgi cell axons are densely immunolabelled in the granule cell layer (G) and their dendrites can be seen in the molecular layer (M). This immunolabelling is completely missing in mGluR2 deficient cerebellum (C). P, Purkinje cell layer. Scale bars: 50 μm.

quickly frozen in liquid nitrogen and thawed in PB, then 70 μm thick sections were cut in the frontal or sagittal plane on a Vibratome. Floating sections were incubated in 20% normal goat serum (NGS) diluted in 50 mM Tris buffer (pH 7.4) containing 0.9% NaCl (TBS) for 1 h. Sections were then incubated overnight or for 24 h, at 4°C in a solution of affinity-purified polyclonal antibodies to either mGluR1α, mGluR2/3 or mGluR5, at a final protein concentration of 1–2.5 μg/ml, diluted in TBS containing 1% NGS. After washes in TBS, the sections were incubated overnight at 4°C in goat anti-rabbit or anti-guinea pig IgG (Fab fragment, diluted 1:50) coupled to 1.4 nm gold (Nanoprobes, Stony Brook, NY) and made up in TBS containing 1% NGS. After several washes in phosphate buffered saline (PBS) the sections were postfixed in 1% glutaraldehyde dissolved in the same buffer for 10 min. They were washed in double distilled water, followed by silver enhancement of the gold particles with an HQ Silver Kit (Nanoprobes) for 8–12 min.

The gold-silver-labelled sections were processed for electron microscopy. This included treatment with OsO_4 (2% in 0.1 M PB) for 40 min, block-staining with uranyl acetate, dehydration in graded series of ethanol, and flat-embedding on glass slides in DURCUPAN (Fluka) resin.

A post-embedding silver-intensified immunogold technique was also used as described earlier (Nusser et al., 1994; Lujan et al., 1996). Ultrathin sections of 70–90 nm in thickness from Lowicryl-embedded blocks (Baude et al., 1993) were picked up on coated nickel grids and incubated for 45 min on drops of blocking solution consisting of 0.8% ovalbumin, 0.1% cold-water fish skin gelatine (Sigma) and 5% fetal calf serum (Sigma) dissolved in PBS. The blocking solution was also used for diluting the primary and secondary antibodies. The grids were transferred to antibodies to mGluR1α (10 μg/ml) or to mGluR2 (mG2Na-5, 20 μg/ml) overnight at room temperature. After washing, the grids were incubated for 2 h on drops of goat anti-rabbit IgG coupled to 1.4 nm gold (Nanoprobes) diluted 1:100 (for mGluR1α, Fab fragment), or goat anti-mouse IgG coupled to 10 nm colloidal gold (for mGluR2, Nanoprobes). Grids were then washed in PBS for 30 min, put on 2% glutaraldehyde in PBS for 2 min and washed in ultrapure water prior to silver enhancement in the dark with an HQ Silver kit for 5 min. Following further washing in ultrapure water, the sections were contrasted for electron microscopy with saturated aqueous uranyl acetate followed by lead citrate.

As controls for method specificity, sections were incubated with the omission of the primary antibodies,

and other sections were incubated with 5% normal rabbit serum replacing the rabbit primary antibodies. Under these conditions, immunoreactivity, resembling that obtained using the specific antibodies, could not be detected. Using a polyclonal rabbit antibody to calretinin (Winsky et al., 1989) no plasma membrane labelling was observed with our pre-embedding method, showing that the labelling found on the plasma membrane is due to the antibodies raised to the peptide sequences present in mGluR1α and mGluR5. Furthermore, using polyclonal rabbit antibodies to synapsin (Naito and Ueda, 1981) no plasma membrane labelling was observed with our post-embedding method, showing that the labelling of the plasma membrane is due to the antibodies raised to the peptide sequence present in mGluR1α. As a control, the mouse monoclonal antibody to mGluR2 was replaced by a monoclonal antibody to glial fibrillary acidic protein (dilution, 1:10, Novocastra, Newcastle upon Tyne, UK). Under these conditions no plasma membrane labelling was seen, but glial fibrillary bundles were strongly labelled.

2.3. Quantification of mGluR1α immunoreactivity on spines following pre-embedding immunogold labelling

The procedure was similar to that used earlier (Lujan et al., 1996). Two samples were taken from the cerebellar molecular layer from two blocks of two animals. Electron microscopic sections were cut from the surface of 70 μm thick sections because immunoreactivity decreased with depth. Randomly taken areas were photographed and printed to a final magnification of $\times 43\,600$ or $\times 45\,400$. Measurements were carried out on 68 micrographs covering a total section area of $\sim 1000\ \mu m^2$. All dendritic spines establishing synapses with parallel fibres were counted and assessed for the presence of immunoparticles; dendritic spines making synapses with climbing fibres were not included in the present study. Only the heads of spines were analysed because spine necks are rarely connected to spine heads in single sections. In the few cases where the neck of a spine was present in the measured section, the natural curvature of the membrane was taken as the continuation of the spine head, cutting off the neck. The length of the synaptic membrane specialisation and the extrasynaptic membrane from all immunopositive spines was measured using a digitising tablet and MACSTEREOLOGY software (Ranforly MicroSystems, UK). The extrasynaptic spine membrane was divided into 60 nm bins. The distance between the closest edge of the postsynaptic density and the centre of the immunoparticles was measured along the spine membrane. Values are given as measurements in the sections; the total tissue shrinkage during the histological processing of such material is ~ 12–19% relative to the living brain (Beaulieu and Colonnier, 1983), but it is not known how the overall shrinkage of the tissue affects the dimensions of the plasma membrane.

In order to compare receptor patterns between material processed by the pre-embedding procedure that involves osmium fixation before dehydration and the post-embedding procedure lacking osmium fixation, it is important that possible differences in shrinkage are estimated, so that a correction can be made to achieve the comparison of equivalent membrane segments. Shrinkage due to processing was compared in the two procedures by measuring the mean sectioned synaptic lengths of parallel fibre synapses following the pre- or post-embedding immunogold reactions. The mean synaptic length obtained from material in the post-embedding reaction (freeze substitution embedding in Lowicryl resin) was 32% smaller than that in pre-embedding reaction (epoxy resin). Therefore, for comparability the measurements obtained with the post-embedding method were multiplied by 1.32.

For the estimation of the mean relative proportion of receptor immunoreactivity in spines, the area of membrane as a function of distance from the synaptic junction was estimated. Since the receptor density changes as a function of distance from the synapse, the amount of receptor at a given distance from the synapse will depend on the receptor density in that position and the area of membrane, which depends on the shape of the postsynaptic element. In order to take into account the change in membrane fraction as a function of distance, spine heads were approximated as spheres and spine necks as cylinders. The average diameter of a spine head and synaptic specialisation was estimated from measurements obtained from serial sections of completely reconstructed spines. The average length of the two longest orthogonal lines that could be fitted in the largest sectioned profile from the series of each spine was used as the diameter of the sphere. For calculating the mean spine head diameter 30 estimated diameters were averaged. The extrasynaptic spine membrane on the sphere was divided into 60 nm wide concentric bins centred around the synaptic junction and the surface areas were calculated for each bin. The mean synaptic junction dimensions were estimated from measurements on 30 serially sectioned synapses. The synaptic specialisation was approximated as a surface segment of one base on the spherical spine head. To obtain an estimate of the mean synaptic base circumference, the section containing the largest dimension of each synapse was chosen from serial sections and the synaptic membrane length was measured accurately along the curvature of the synapse. One half of the mean synapse length was used as the length of the shortest line (l) connecting the pole of the spherical spine head with a point in the base of the surface segment along the surface. From the diameter of the sphere and l the circumference of the base could be calculated.

2.4. Quantification of mGluR2 immunoreactivity on dendritic shafts and axon terminals

Two samples were taken from the cerebellar molecular layer from one block. As described above for mGluR1α, electron microscopic sections were obtained from a thick section close to the surface where immunoreactivity was strongest. Two Golgi cell dendrites immunolabelled by antibodies to mGluR2/3 were identified, photographed in serial sections and printed to a final magnification of $\times 62\,500$. Dendritic spines usually make only one synaptic junction and therefore the most likely source of glutamate that might be relevant for the receptors on the spine can be predicted. In contrast, it is much less obvious which, if any, of the synapses on the smooth dendritic shafts of Golgi cells could act as a source of glutamate for receptors scattered along the dendritic membrane. In single EM sections of dendritic shafts it is not possible to measure the distance of a receptor to the nearest synapse, because synapses in all directions have to be considered. Therefore, three dimensional reconstructions were carried out from 25 sections covering a length of ~ 2 μm for each dendrite. For graphical presentations, reconstructions were carried out using MACSTEREOLOGY software (Ranforly Microsystems, UK). Two physical models were also constructed to scale by tracing the outline of each sectioned profile onto board of appropriate thickness, estimating EM section thickness as 80 nm. The distance between the closest edge of the nearest postsynaptic density and the centre of the immunoparticles present in the dendritic shaft was measured along the dendritic surface on the physical models. The measurements are presented in relation to the synaptic junctions present in the reconstructed dendritic segments. It is possible that some of the particles close to the cut ends of the dendritic segments were closer to synapses outside the reconstructed segments, therefore the estimates may be slightly biased for larger values. However, the conclusion of the analysis is not affected by this possible overestimation of the distance for a fraction of the particles.

We tested whether the construction of physical models may be replaced by a mathematical estimation of the distance of receptor immunoparticles to the closest synaptic junction. The more regularly shaped dendrite (D1) was approximated by a stack of two cylinders. The shape of dendrite D2 was irregular, therefore measurements by cylindrical approximation could not be applied. For the mathematical approximation each serial EM section was superimposed in a correct 3D position for which a general co-ordinate reference system was established. The position of every gold particle and synapse was measured relative to this reference system. The perimeter of the dendrite on every section was approximated by the closest circle, which also was used to determine the diameter and position of the optimal cylinder. The position of gold particles was changed to fit the cylinder using radial projection. Finally, the surface of the cylinder was rolled out and the distances between gold particles and the edge of each synapse were measured and the shortest distance was used in statistical analysis.

For quantification of mGluR2 on axon terminals, Golgi cell boutons immunoreactive for mGluR2 were identified, photographed on single or serial sections and printed to a final magnification of $\times 33\,000$. Measurements were carried out on a total section area of approximately 400 μm^2. All vesicle-containing Golgi cell axon profiles in apposition with granule cell dendrites were assessed for the presence of immunoparticles, regardless of whether they formed synaptic contact. The number of immunogold particles present in the extrasynaptic membrane of the axon terminals, in the presynaptic grid of synapses formed with granule cell dendrites and within the terminal away from the plasma membrane was counted. Data are expressed as percentages of immunoparticles in each compartment.

2.5. Quantification of mGluR5-immunoreactive spines

For calculating the mean distribution of the receptor on spines, the same data set that has already been published (Lujan et al., 1996) was re-analysed and a new data set was also collected from serial sections. For the estimation of the relative proportion of receptor immunoreactivity at different positions in spines, the area of membrane as a function of distance from the synaptic junction was estimated by approximating spine heads with spheres and spine necks with cylinders, as described above. The mean estimated diameter of 30 spine heads was obtained from serial sections.

For the characterisation of individual spines by serial section analysis, nine new areas of strata oriens or radiatum of the CA1 area were sampled from two blocks of two animals. The same area was photographed in five to twelve serial sections in each sample and printed to a final magnification of $\times 33{,}500$, covering a total tissue volume of ~ 200 μm^3. Dendritic spines in a section from the middle of the series from strata oriens (16–28 per series; total of 90) and radiatum (25–32 per series; total of 115) were numbered and then followed through serial sections in both directions as long as the synaptic specialisation was detected. All profiles of each immunopositive dendritic spine with a clear synaptic specialisation were assessed, but only spines with completely reconstructed synaptic densities were included in the analysis. The number of immunoparticles on the spine membrane was counted and the proportion of particles within 60 nm of the edge of the active zone was established. In addition the position of each particle was measured within the individual

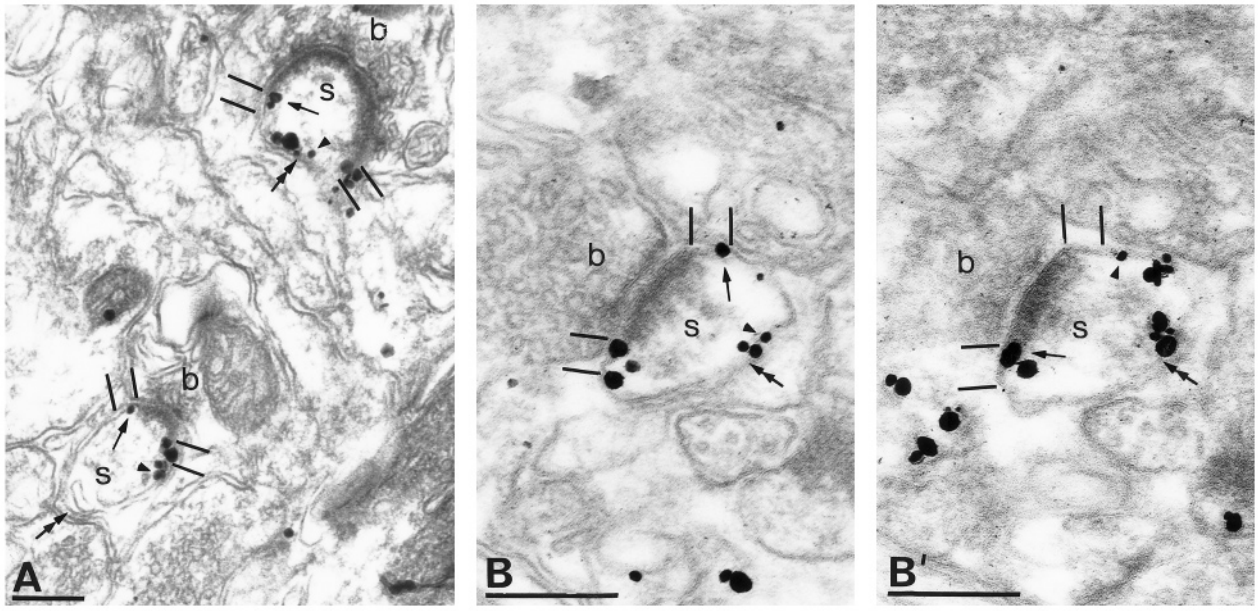

Fig. 2. Electron micrographs showing immunoreactivity for mGluR1α in the molecular layer of the cerebellar cortex (A) and mGluR5 in the hippocampal CA1 area (B and B′, serial sections), as demonstrated by pre-embedding silver intensified immunogold labelling. (A) Immunogold particles are located at the edge of the synaptic specialisation (e.g. arrows) and also at some distance from the synapse (e.g. arrowheads) on Purkinje cell spines (s). (B and B′) An axon terminal (b) in stratum radiatum establishes a synapse with a pyramidal cell spine (s) which contains particles (e.g. arrows) surrounding the postsynaptic membrane specialisation and also along the extrasynaptic spine membrane (e.g. arrowheads). The perisynaptic 60 nm wide segments of the plasma membrane are indicated by bars, and the half distance in the perimeter of extrasynaptic spine membrane by double arrows. Scale bars: 0.2 μm.

sections with respect to the edge of the postsynaptic density.

2.6. Display of data and statistics

The Kolmogorov–Smirnov non-parametric test was used to examine whether samples taken for each mGluR were from a homogeneous population. The grouped data for the three mGluRs were also compared to each other using the Kolmogorov–Smirnov test and the same test was used to compare spine populations for the location of mGluR5. All remaining statistical comparisons were done using the Mann–Whitney test. The differences were considered significant at the level of $P < 0.05$. Data are presented as mean $\pm$ S.D.

3. Results

3.1. Pattern of distribution of immunoreactive mGluRs in the plasma membrane as revealed by pre-embedding reactions

Since the antibodies are applied to 70 μm thick sections, the strength of labelling decreases with depth and antibodies may penetrate unevenly into the tissue depending on the microenvironment. Therefore, at any given depth in the thick section, only immunolabelled structures can be compared because some structures that contain the receptor may remain unlabelled due to the limited antibody penetration. Variability amongst labelled structures may also be partly a result of differential antibody penetration. The post-embedding procedure overcomes these problems, but it is less sensitive and in the present project could not be applied equally to all three receptors.

The pre-embedding silver-intensified immunogold method resulted in a non-diffusible label which was mainly associated with plasma membranes for all three mGluRs (Figs. 2 and 3). As reported previously (Baude et al., 1993; Nusser et al., 1994), immunoparticles were located on the intracellular surface of the plasma membrane (Figs. 2 and 3), which confirms the predicted intracellular location of the C-terminal part of mGluR1α, mGluR2/3 and mGluR5, supporting the predicted transmembrane topology of the receptors as deduced from the amino acid sequence (Masu et al., 1991; Abe et al., 1992; Tanabe et al., 1992).

mGluR1α and mGluR5: In the cerebellar molecular layer, presynaptic boutons containing few or no mitochondrial profiles and establishing single asymmetric axo-spinous synapses on Purkinje cells were considered to originate from parallel fibres (Peters et al., 1991). As reported previously (Baude et al., 1993; Nusser et al., 1994), immunolabelling for mGluR1α in Purkinje cell spines showed an enrichment of receptor in a perisy-

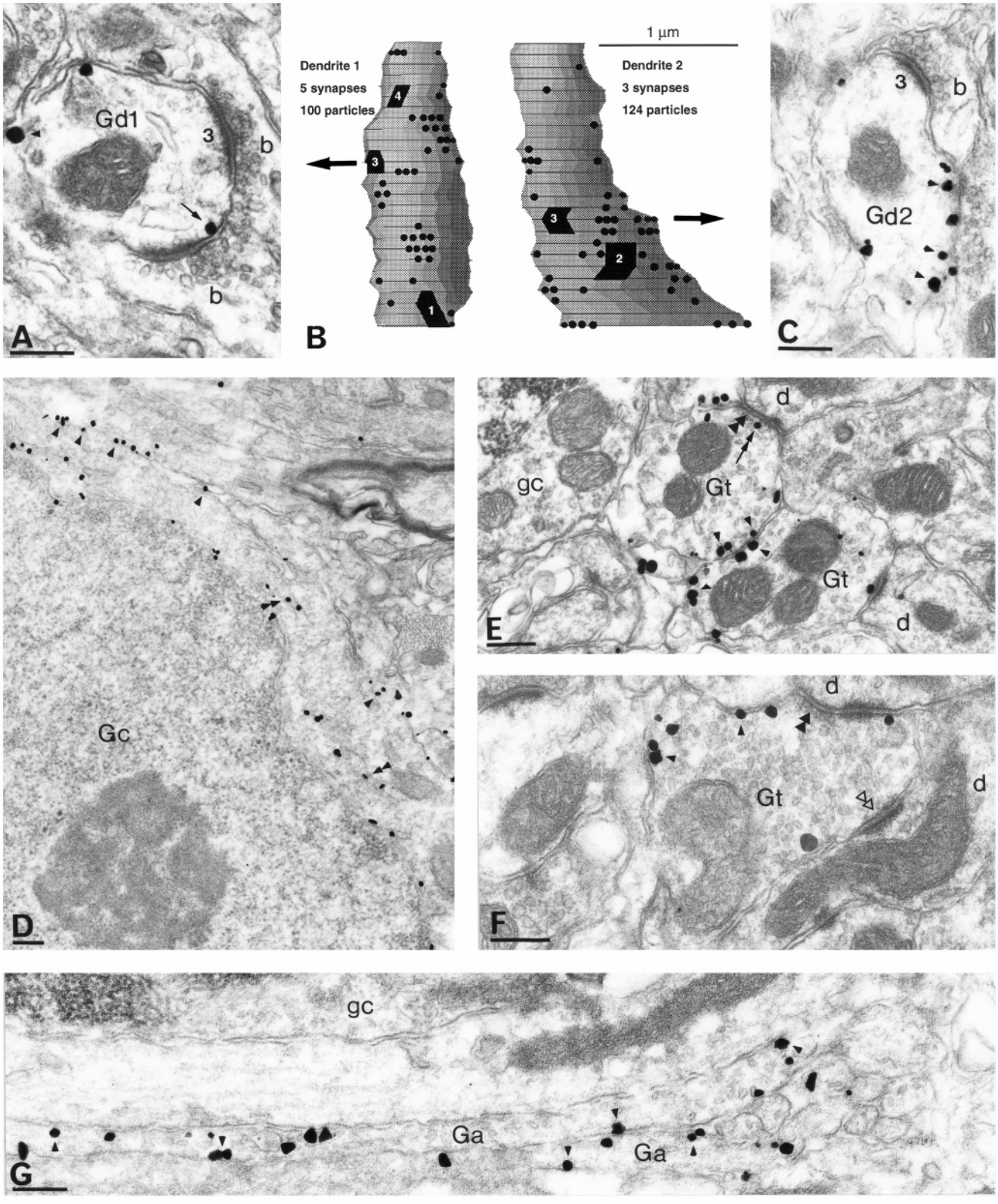
Gd1
3
b
b
A
Dendrite 1
5 synapses
100 particles
4
3
1
B
1 µm
Dendrite 2
3 synapses
124 particles
3
2
3
b
Gd2
C
Gc
D
gc
Gt
d
Gt
d
E
Gt
d
d
F
gc
Ga
Ga
G

Fig. 3.

naptic position (0–60 nm), but labelling was also present throughout the extrasynaptic (60–900 nm) membrane (Fig. 2A). In the hippocampal CA1 area, axon terminals make asymmetric axo-spinous synapses on pyramidal cells and immunolabelling for mGluR5 could be found both perisynaptically and extrasynaptically on these postsynaptic spines (Lujan et al., 1996 and see also Fig. 2B and B′). The pattern was consistent in different sections of the same spines as visualised through serial sections (Fig. 2B and B′). However, some other mGluR5-immunoreactive spines lacked immunoparticles at the perisynaptic sites, but were labelled on the extrasynaptic membrane.

mGluR2: Golgi cells of the cerebellar cortex are some of the most strongly labelled neurons for group II mGluRs in the brain (Ohishi et al., 1993a), therefore they were chosen for comparison with group I mGluR-containing cells. In situ hybridisation results show that Golgi cells express mainly mGluR2 and to a small extent mGluR3 (Ohishi et al., 1993a,b). Although the antibody used in the present study weakly recognises mGluR3 in addition to strongly reacting with mGluR2, it is likely that the labelling is mainly or exclusively due to mGluR2. This conclusion is supported by the observation that in mGluR2 knock-out mice this antibody failed to reveal Golgi cells, although strong labelling was obtained in wild type mice (Fig. 1).

The molecular layer contained smooth, radial dendrites labelled for mGluR2 as revealed by electron microscopy. Based on the previous (Ohishi et al., 1993a) and the present light microscopic results showing that only the dendrites of Golgi cells were labelled strongly with this antibody in the molecular layer, we assumed that the dendrites analysed in the electron microscope belonged to Golgi cells, although they could not be traced to cell bodies in the granule cell layer. Immunolabelling for mGluR2 was found throughout the dendritic shafts (Fig. 3B and C), which received input from parallel fibres. Immunoparticles were found occasionally at the edge of synaptic specialisations (Fig. 3A), although most of them were present throughout the extrasynaptic dendritic membrane, often in clusters (e.g. D1 in Fig. 3B). Immunoparticles for mGluR2 could also be seen outlining the somatic plasma membrane and the endoplasmic reticulum cisternae including the nuclear envelope of some Golgi cells (Fig. 3D). As described earlier (Ohishi et al., 1994), Golgi cells were also immunolabelled along their axons and boutons (Fig. 3E–G). Out of a total of 350 immunoparticles associated with vesicle-containing bouton profiles, 79% were located along the plasma membrane at various distances from the synaptic junction (Fig. 3E and F), 2% were found on the presynaptic grid of both symmetrical and asymmetrical synapses (Fig. 3E), and 19% of immunoparticles within the terminals were not associated with the plasma membrane. In many cases these intraterminal particles were associated with the smooth endoplasmic reticulum (ER) tubules, but because of the small diameter of the tubules and the relatively large size of the particles, the smooth ER could not be identified in every case. Since the ER tends to occur frequently near mitochondria, the intraterminal particles also often followed the outline of mitochondria.

3.2. Validation of the pre-embedding immunocytochemical procedure for quantification

In order to exclude the possibility that the patterns of receptor distribution are biased by limitations of the pre-embedding immunocytochemical method, which has been shown to be inadequate to reveal some receptors within the synaptic junction (Baude et al., 1995; Nusser et al., 1995), the distributions of mGluR1α on spines of Purkinje cells was also studied using the post-embedding method. This receptor and the antibody recognising it were chosen for the comparison because, out of the three receptors studied here, the highest level of labelling was obtained for mGluR1α. Measurements were carried out on micrographs in the same way from material obtained by either method and correction was made for differential shrinkage to ensure the comparison of equivalent plasma membrane areas.

Labelling using the post-embedding method was always weaker than that observed using the pre-embedding technique, as revealed by the difference in the absolute number of immunoparticles per spine in individual sections (post-embedding reaction, 2.25 ± 1.15 particles/spine; pre-embedding reaction 3.16 ± 1.80 particles/spine). However, the distributions of immunopar-

Fig. 3. Immunoreactivity for mGluR2 in Golgi cells in the cerebellar cortex as demonstrated by pre-embedding silver intensified immunogold labelling. (A and C) Two different Golgi cell dendritic shafts (Gd1 and Gd2) receiving synapses from parallel fibre terminals (b). Immunoparticles were rarely found at the edge of the synaptic junctions (arrow); most particles were at the dendritic membrane away from synapses (e.g. arrowheads), often in groups. (B) Reconstruction ($n = 25$ sections) of two Golgi cell dendrites from serial sections showing the position of immunoreactive mGluR2 in relation to parallel fibre synapses (numbered; the other synapses are on the back of the dendrites). Arrows indicate the EM sections illustrated in A and C. Synapses numbered 3 in A and C correspond to synaptic specialisation seen in B. (D) Non-synaptic areas along the somatic membrane (e.g. arrowheads) and the endoplasmic reticulum (e.g. double arrowheads), including the nuclear envelope, of some Golgi cells (Gc) were also labelled. (E and F) Golgi cell axon terminals (Gt) making symmetrical (double filled triangles) and asymmetrical (double open triangles) synapses with granule cell dendrites (d). Immunoparticles were occasionally located in the presynaptic grid (double arrow), but most of them were found away from the synaptic junction (e.g. arrowheads). (G) Axons of Golgi cells (Ga) were also heavily immunolabelled for mGluR2 along the plasma membrane (e.g. arrowheads). gc, granule cell. Scale bars: 0.2 μm.

ticles (Fig. 4) detected with the two methods did not differ from each other ($P > 0.08$), confirming that the quantitative results obtained with the pre-embedding method are not biased by the differential accessibility of the epitopes.

To our knowledge, the detection of group II mGluRs has not been reported with the post-embedding method, therefore we also validated the pre-embedding results for mGluR2. Unfortunately, in spite of trying many different post-embedding conditions no signal was obtained with the guinea pig antibody. However, the recently developed monoclonal antibody to mGluR2 selectively labelled a few interneuron dendrites in the molecular layer and also labelled thin axons and Golgi cell terminals in the granular layer (not illustrated). None of the seven parallel fibre synapses seen on mGluR2 labelled dendrites had gold particles over the synaptic membrane specialisation, but the extrasynaptic plasma membrane was sparsely labelled, in agreement with the results of the pre-embedding reaction. The signal in the post-embedding reaction was weaker, therefore the pre-embedding material was used for measurements.

3.3. Quantitative comparison of the location of mGluRs

To establish the relative densities of postsynaptic mGluR1α, mGluR5 and mGluR2 in relation to glutamate release sites, measurements were taken from single and serial EM sections. The measurements for mGluR5 are taken from our previous work (Lujan et al., 1996) and re-analysed here for comparison with the other two mGluRs. The position of immunoparticles (mGluR1α, $n = 332$; mGluR5, $n = 345$; mGluR2, $n = 218$) was measured from the closest edge of the nearest synaptic specialisation. Equidistant membrane segments on opposite sides of a synaptic junction correspond to an annulus centred on the synapse, therefore for the display of the data the measurements from the two sides are pooled. Data are displayed as frequency of particles in arbitrarily chosen 60 nm wide segments of the membrane of dendritic spines and shafts, starting at the edge of the synaptic membrane specialisation. Two samples, one each from two animals, were analysed for mGluR1α and two Golgi cell dendrites from one block were measured for mGluR2. Since the distributions in the two samples for each receptor did not differ from each other (Kolmogorov–Smirnov test, $P > 0.16$, mGluR1α; $P > 0.67$, mGluR2), the data were pooled. In a total measured area of $\sim 1000\ \mu m^2$ of the cerebellar molecular layer, 108 immunopositive Purkinje cell spines exhibiting synaptic specialisation in a single section were encountered. The mean length of the synaptic membrane specialisation of the immunopositive Purkinje cell spines ($n = 108$) was 279.3 ± 94.5 nm as measured from single sections that randomly cut the synaptic junction, therefore the value does not represent the maximum dimension of the synapse. The synaptic junctions on Golgi cell dendrites were completely reconstructed and had a mean largest dimension of 169.4 ± 43.7 nm ($n = 8$).

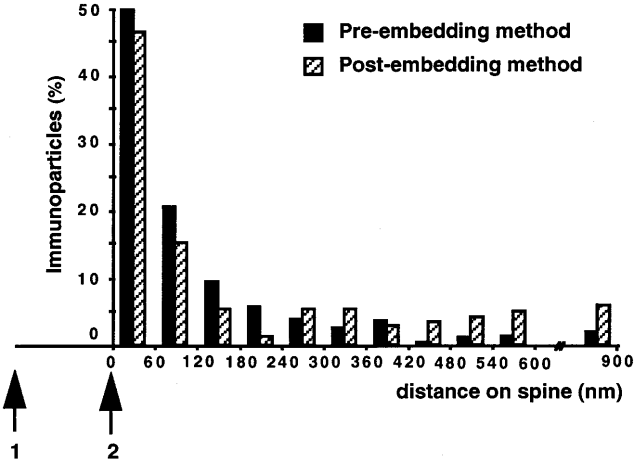

Fig. 4. Comparison of pre-embedding ($n = 108$ spines; solid columns) and a post-embedding ($n = 64$ spines; striped columns) immunogold methods for characterising the distribution of immunoreactive mGluR1α on spine heads of cerebellar Purkinje cells in relation to the postsynaptic membrane specialisations (arrows). Measurements using either methods resulted in a similar distribution ($P > 0.08$), showing that mGluR1α is strongly concentrated in a perisynaptic annulus surrounding the postsynaptic membrane specialisation. Arrows 1 and 2 mark respectively, the middle and the edge of the average length of synaptic junction as measured in individual sections.

The perimeter of the Purkinje cell spines appearing in a section greatly varies from one spine to another (mean 1055.1 ± 346.8 nm, extrasynaptic membrane only) due to the variation in the size of spines and in the plane of the section. In the comparison of different mGluRs, the relative density of receptor in the plasma membrane as a function of distance from the transmitter release site is an important parameter. Since measurements on spines could only be taken if they had the synaptic junction in the plane of the section, the sample was enriched in membrane close to the synapse. Therefore, to compensate for the under-representation of distal spine membrane, the counts of immunoparticles were normalised to the observed relative frequency of the 60 nm membrane segments at a given distance in the sampled spine population (Fig. 5A and B). The data expressed in this way show the change in density of receptor as a function of distance from the synapse.

Depending on the shape of the spines and the area occupied by the synaptic specialisation, concentric segments of equal width of spine membrane, which were used for binning the data, represent different areas of membrane. Since we wanted to determine and compare the relative size of receptor pools at a given distance from the transmitter release site, it is necessary to normalise the data for the area of membrane at a given distance. This is difficult to do for each single spine in the absence of full 3D reconstruction, because their shapes are very

different. Therefore, as a first approximation we made a normalisation for an average spine represented by a spherical head and a cylindrical neck. The mean head diameters were estimated from serial sections and they were 349.7 ± 52.2 nm for Purkinje cell spine heads with a neck of 174.6 nm in diameter and 281.2 ± 79.8 nm for pyramidal cell spine heads with a neck of 91.3 nm in diameter (Fig. 5A′ and B′). The neck diameters are not based on measurements: they were arbitrarily chosen to coincide with the base of a 60 nm membrane segment closest in diameter to 100 nm, a dimension that is in the range of observed spine neck diameters. The normalisation also required an estimate of the mean synaptic junction dimension in order to calculate the circumference of the base of the perisynaptic membrane segment. The synaptic specialisation was approximated by a surface segment of one base on the spherical spine head. The mean synaptic membrane specialisation length (measured along the largest extent in the plane of sections that randomly cut the synapses) was 316.0 ± 79.0 nm for Purkinje cell spines and 189.6 ± 52.1 nm for pyramidal cell spines.

Immunogold particles for mGluR1α had the highest density in a perisynaptic position (Fig. 5A) where 90% of immunoreactive spines were labelled within 60 nm of the edge of the synaptic junction. Since the synaptic specialisation occupied a substantial segment of the spine head, the absolute membrane area per bin changed relatively little within 240 nm from the edge of the synapse, therefore the skewed receptor density distribution resulted in a skewed distribution of the absolute amount of receptor (c.f. Fig. 5A and A′). Following normalisation for the membrane area, it is apparent that about 50% of all receptor immunoparticles are within 60 nm of the synaptic membrane specialisation. Immunoparticle concentration and fraction dropped markedly as a function of distances from the synapse. The density of mGluR5 was also highest in a perisynaptic annulus (Fig. 5B), but in contrast to mGluR1, receptor density remained relatively uniform in the 240 nm band around the synapse. Since the dimension of the average synaptic specialisation is smaller on pyramidal cells than on Purkinje cells (see above), the area of the first membrane segment around the synapse is smaller than the subsequent three segments. Therefore, after normalisation for membrane areas (Fig. 5B′), the level of receptor labelling is closer between 60–240 nm to that of the first 60 nm membrane segment. Nevertheless, about 25% of immunolabelled mGluR5 is associated with the immediate edge of the synapse, followed by about 50% of all receptors on spines in a 60–240 nm wide band (Fig. 5B′). The receptor density and fraction appear to decrease markedly further in the spine membrane.

In contrast to group I mGluRs, immunoparticles for mGluR2 were not associated with the glutamatergic parallel fibre synapses, but were distributed throughout the plasma membrane separating different synaptic junctions on the dendritic shafts (Fig. 5C). Because of the differences of distances between synapses on Golgi cell dendrites, no attempt was made to calculate the membrane areas at a given distance. Nevertheless, it can be predicted that the apparent increase in receptor fraction away from the synapses (Fig. 5C) reflects the increase of membrane area between 180–420 nm from synapses. The proportion of immunoparticles at distances larger than 600 nm (Fig. 5C) may not be representative because some of the particles could be close to synaptic junctions present outside the dendritic segment that was included in the EM reconstruction for quantification.

The distributions of immunoparticles for the three mGluRs were compared pairwise and differences between each of them were found to be significant (Kolmogorov–Smirnov test, $P < 0.0001$ in each case). A representation of the distribution of mGluRs that avoids possible binning artefacts is achieved by using cumulative probabilities which allow a comparison to hypothetical distributions as shown in Fig. 6. The steep slope of the cumulative probability curve for mGluR1α (Fig. 6A) reflects the tight association of the receptor with positions very close to the synaptic membrane specialisation. The cumulative probability curve for the mGluR5 (Fig. 6B) also has a pronounced initial slope, but it becomes less steep than that for mGluR1α (see also Section 3.4). A second change in the slope at around 250 nm demonstrates that overall pyramidal spines have three levels of mGluR5 in their membrane. In the case of mGluR2, the distribution of immunoparticles for dendrite D1 measured on the physical model and calculated by a cylindrical approximation of the dendrite surface was not significantly different ($P > 0.74$, Fig. 6C). The probability curve has a smooth and uniform slope along the whole distance on the dendrite (Fig. 6C). The distributions on the two dendrites were not different ($P > 0.67$).

To test to what degree the distribution of immunoparticles in the plasma membrane relative to the synaptic junction differed from random distribution, random distributions were generated for the same number of gold particles over the same membrane length. The averages of randomly generated receptor positions from ten simulations are shown in Fig. 6. The distributions of mGluR1α and mGluR5 differed significantly from random distribution (Kolmogorov–Smirnov test, $P < 0.0001$ and < 0.002, respectively), whereas the distribution for mGluR2 did not differ

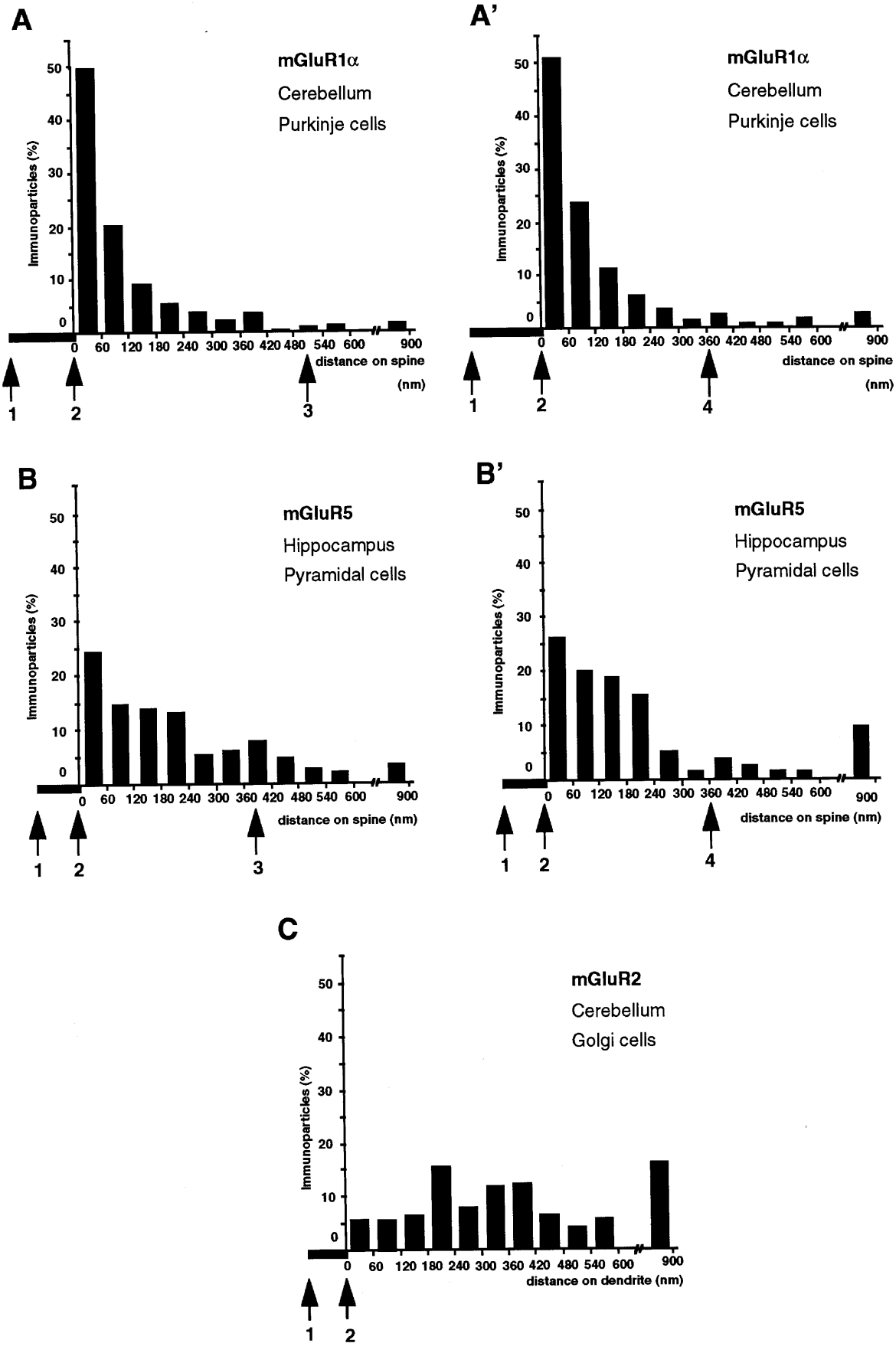
A
mGluR1α
Cerebellum
Purkinje cells
Immunoparticles (%)
0 10 20 30 40 50
0 60 120 180 240 300 360 420 480 540 600 900
distance on spine (nm)
1 2 3
A'
mGluR1α
Cerebellum
Purkinje cells
Immunoparticles (%)
0 10 20 30 40 50
0 60 120 180 240 300 360 420 480 540 600 900
distance on spine (nm)
1 2 4
B
mGluR5
Hippocampus
Pyramidal cells
Immunoparticles (%)
0 10 20 30 40 50
0 60 120 180 240 300 360 420 480 540 600 900
distance on spine (nm)
1 2 3
B'
mGluR5
Hippocampus
Pyramidal cells
Immunoparticles (%)
0 10 20 30 40 50
0 60 120 180 240 300 360 420 480 540 600 900
distance on spine (nm)
1 2 4
C
mGluR2
Cerebellum
Golgi cells
Immunoparticles (%)
0 10 20 30 40 50
0 60 120 180 240 300 360 420 480 540 600 900
distance on dendrite (nm)
1 2

Fig. 5.

from random distribution ($P > 0.07$, physical model; $P > 0.24$, cylindrical approximation).

3.4. Heterogeneity of mGluR5-immunoreactive spines on pyramidal cells

When the distribution of the pooled population of mGluR5 on pyramidal spines was compared to mGluR1α on spines of Purkinje cells, the former was significantly less tightly aligned to the synaptic junctions. We tested whether this pattern was a result of all pyramidal spines having less perisynaptic and more extrasynaptic receptors, or if the perisynaptic receptor pool was missing from some spines, as it appeared from single sections (see e.g. Fig. 2C in Lujan et al., 1996). The serial section analysis also helped to measure the fraction of immunopositive spine population which was between 70–85% of the total spine population at a given depth within the block. Measurements were taken from nine samples of five to 12 serial EM sections each, in strata oriens and radiatum. Although the samples from the two strata did not differ from each other (Kolmogorov–Smirnov test, $P > 0.1$) data were not pooled, because strata oriens and radiatum receive partly different glutamatergic inputs. All dendritic spines ($n = 90$, stratum oriens; $n = 115$, stratum radiatum) were included in the sample from the photographed areas if all their sectioned profiles having a clear synaptic membrane specialisation were in the sectioned volume. Because the position of particles relative to the synaptic junction could not be measured in the sections where the synaptic junction disappeared, the immunoparticles were not counted in the sectioned profiles of the same spines which had no synaptic specialisation. In stratum oriens, 61 spines (68%) were immunopositive using the criterion of at least one particle associated with the spine membrane. In stratum radiatum, 99 spines (86%) were immunopositive, but with the pre-embedding method the two strata cannot be compared. From 236 gold particles on spines in stratum oriens, 44 (18.6%) were in perisynaptic position. In stratum radiatum, from 410 particles counted on spines, 121 (29.5%) were in perisynaptic position. The position of mGluR5 in the membrane of the pooled spine population relative to the synaptic junction was significantly different (Kolmogorov–Smirnov test, $P < 0.0001$) from random distribution (Fig. 7B), but not different ($P > 0.07$) from the other sample obtained from single sections and presented in Section 3.3.

The distribution of mGluR5-immunoreactive dendritic spines (Fig. 7) appears to be heterogeneous with respect to the ratio of perisynaptic versus extrasynaptic mGluR5 pools in both strata oriens and radiatum. Thus, approximately half of the immunopositive dendritic spines had no immunogold particles in the perisynaptic position whereas others were labelled at both perisynaptic and extrasynaptic positions (Fig. 7A). The proportion of immunoparticles within 60 nm of the active zone was variable (Fig. 7A). To determine whether the heterogeneity between spines was due to differences in labelling intensity, perhaps caused by technical factors, comparisons were carried out between populations of spines. The number of gold particles in spines having or lacking mGluR5 in perisynaptic sites did not differ from each other either in stratum oriens (4.29 ± 2.40 particles and 3.54 ± 2.36 particles, respectively; Mann–Whitney test, $P > 0.1$) or in stratum radiatum (4.53 ± 2.87 particles and 3.58 ± 2.37 particles, respectively; Mann–Whitney test, $P > 0.7$). However, when spines containing immunoparticles only within 60 nm of the active zone were compared to the other spines containing receptors in perisynaptic locations, a significant difference was found in stratum radiatum (1.73 ± 0.65 vs 5.14 ± 2.81 particles, respectively; Mann–Whitney test, $P < 0.0001$). The trend was similar in stratum oriens, but the difference was not significant (3.00 ± 1.15 and 4.50 ± 2.50 particles, respectively; Mann–Whitney test, $P > 0.24$). The exclusively perisynaptic labelling in spines that are labelled by few particles, might reflect the preferential reaction of antibodies with sites of high receptor density when only a limited number of antibodies penetrate into a spine, i.e. the receptor may be in the spine membrane at several sites,

Fig. 5. Distribution of immunoreactive mGluRs in relation to glutamate release sites as assessed from immunogold reactions (see Figs. 2 and 3). (A and A′) Spine heads ($n = 108$) of cerebellar Purkinje cells. (B and B′) Spine heads ($n = 207$) of hippocampal CA1 pyramidal cells (stratum radiatum). (C) Dendrites ($n = 2$) of cerebellar Golgi cells. Arrows mark the middle (1) and the edge (2) of the average length of the postsynaptic membrane specialisations on each structure. Arrow 3 marks the half distance of extrasynaptic membrane perimeter of the average spine as measured from electron micrographs (see Fig. 2). (A and B) Immunoparticles were recorded in 60 nm wide bins along the extrasynaptic plasma membrane. (A′ and B′) The same data displayed after normalisation for membrane area by approximating the shape of spine heads as spheres and the spine neck as cylinders. Arrow 4 marks the distance along the spine membrane at the start of the cylindrical spine neck in the approximation. Data are expressed as the proportion of immunoparticles at a given distance from the edge of the synaptic specialisation. The measurements show that mGluR1α is more strongly concentrated in a perisynaptic annulus surrounding the postsynaptic specialisation than mGluR5 which is distributed at high density in a broader membrane segment. In contrast to the above two group I mGluRs, mGluR2 is not associated with glutamatergic synapses in the dendritic plasma membrane of cerebellar Golgi cells (data not normalised for membrane area, all distances of immunoparticles measured on physical model).

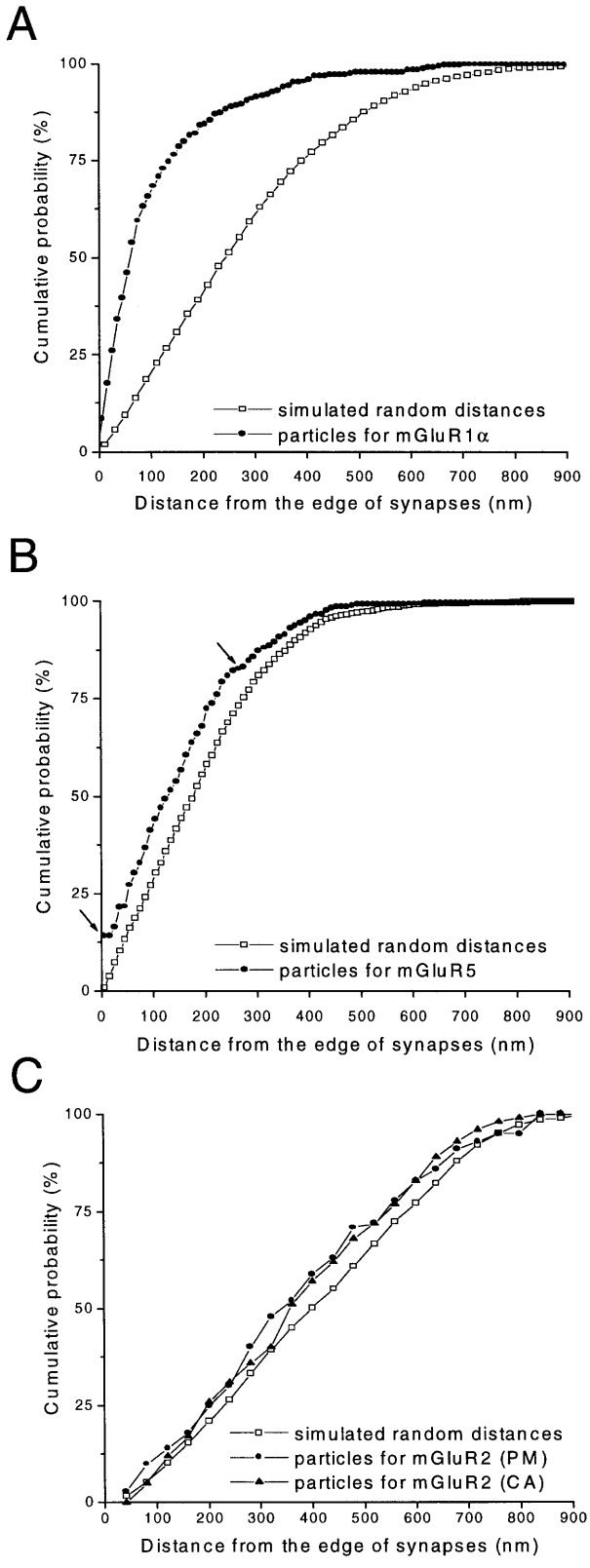

Fig. 6.

but at different concentration, and only the highest concentration is revealed by immunoreaction. However, the genuinely exclusive concentration of receptor at the edge of the synapse cannot be excluded.

It follows from the above that the average distribution of mGluR5 in spines does not appear in individual spines. Therefore, to see whether the distribution of mGluR5 in pyramidal spines that have perisynaptic receptor is the same as the distribution of mGluR1α, in Purkinje cell spines which almost always exhibit perisynaptic receptor, comparisons were made between the distributions of receptor populations. Even after selecting only pyramidal spines that showed some perisynaptic mGluR5, the receptor distribution is significantly different from that of mGluR1α, (Kolmogorov–Smirnov test, $P < 0.0003$). The difference results from the higher proportion of mGluR1α in perisynaptic position, as opposed to the higher fraction of extrasynaptic mGluR5 in the 60–240 nm membrane band of pyramidal spines (Fig. 7B). Interestingly, when the distribution of mGluR5 is compared only in the 60–900 nm membrane band of pyramidal spines with or without perisynaptic labelling (0–60 nm band), the distributions are not different (Kolmogorov–Smirnov test, $P > 0.16$). It therefore appears that the fraction of receptor, present in the perisynaptic position of some spines having a perisynaptic pool, is evenly distributed in the extrasynaptic membrane of other spines that lack the perisynaptic pool.

4. Discussion

The application of quantitative immunocytochemistry has demonstrated that each of the three receptors, mGluR1α, mGluR5 and mGluR2 have a unique distribution in the somato-dendritic plasma membrane domain of neurons in relation to glutamate release sites. Group I mGluRs are concentrated to a differing degree in a perisynaptic position, whereas mGluR2 does not appear to be associated spatially with synaptic inputs.

Fig. 6. Comparison of the distribution of immunoreactive mGluRs (solid symbols) to simulated random distribution (open squares, average of $n = 10$) of receptor immunoparticles on the same population of postsynaptic profiles. Data are expressed as cumulative probability of occurrence at a given distance from the edge of the synaptic specialisation. The distribution of immunoparticles for mGluR1α and mGluR5, differ significantly from random distribution (Kolmogorov–Smirnov test, $P < 0.0001$ and < 0.002, respectively) on the same membrane surface. In contrast, the distribution of immunoparticles for mGluR2, measured in two different ways on a Golgi dendrite, did not differ from the simulated distribution of randomly placed receptors (Kolmogorov–Smirnov test, $P > 0.24$, cylindrical approximation [CA]; $P > 0.07$, physical model [PM]). Arrows in B indicate the points of change in the slope of the curve showing the distribution of mGluR5.

Since all three receptor subtypes were found outside the synaptic membrane specialisation, the previous suggestion (Baude et al., 1993) that their location reflects their differential activation in an activity dependent manner seems to apply to all mGluRs in the somato-dendritic domain. Furthermore, considering that their affinity is higher for glutamate than that of the synaptic AMPA type receptors, the location outside the synaptic junction decreases the likelyhood of receptor desensitization, maintaining their role in activity-dependent processes. The measurements were carried out on three different cell types in two brain areas, therefore both the subtype of mGluR and factors associated with the cell type could have influenced the patterns of distribution. We have not been able to identify a cell type which expresses several subtypes of postsynaptic mGluR at sufficiently high concentration to enable a comparison of distributions with the immunogold technique, therefore we compared the three receptors on different cell types.

4.1. Methodological considerations

With regard to the qualitative pattern of receptor distribution the results of the pre-embedding immunogold localisation of mGluR1 and mGluR5 are in agreement with both the results obtained with the post-embedding method (Baude et al., 1993; Nusser et al., 1994; Lujan et al., 1996) and those obtained in other brain areas (Vidnyanszky et al., 1994, 1996). However they are at variance with the results of electron microscopic immunoperoxidase studies which show a dense labelling of the postsynaptic membrane specialisation (Martin et al., 1992; van den Pol, 1994; Romano et al., 1995; van den Pol et al., 1995). We could reproduce such a labelling with our antibodies (Baude et al., 1993; Lujan et al., 1996) and interpreted it as showing the diffusion of the peroxidase reaction product from peri- and extrasynaptic sites, followed by secondary deposition on the postsynaptic density. This interpretation and the perisynaptic location of the receptors have been questioned on the basis of the immunoperoxidase results (van den Pol et al., 1995), but no experimental evidence has been offered to exclude the diffusion of the peroxidase reaction product. Group II and III mGluRs have also been suggested to be in the postsynaptic membrane specialisation (Bradley et al., 1996; Petralia et al., 1996), but again, until such a localisation can be demonstrated with a particulate marker, the most parsimonious interpretation of the immunoperoxidase results is that the reaction product is deposited secondarily on the postsynaptic density, and the main body of the postsynaptic density lacks mGluRs.

As discussed earlier (Baude et al., 1995; Lujan et al., 1996; Matsubara et al., 1996), for a high resolution quantitative evaluation of membrane receptors, the post-embedding immunogold method is preferred, because all

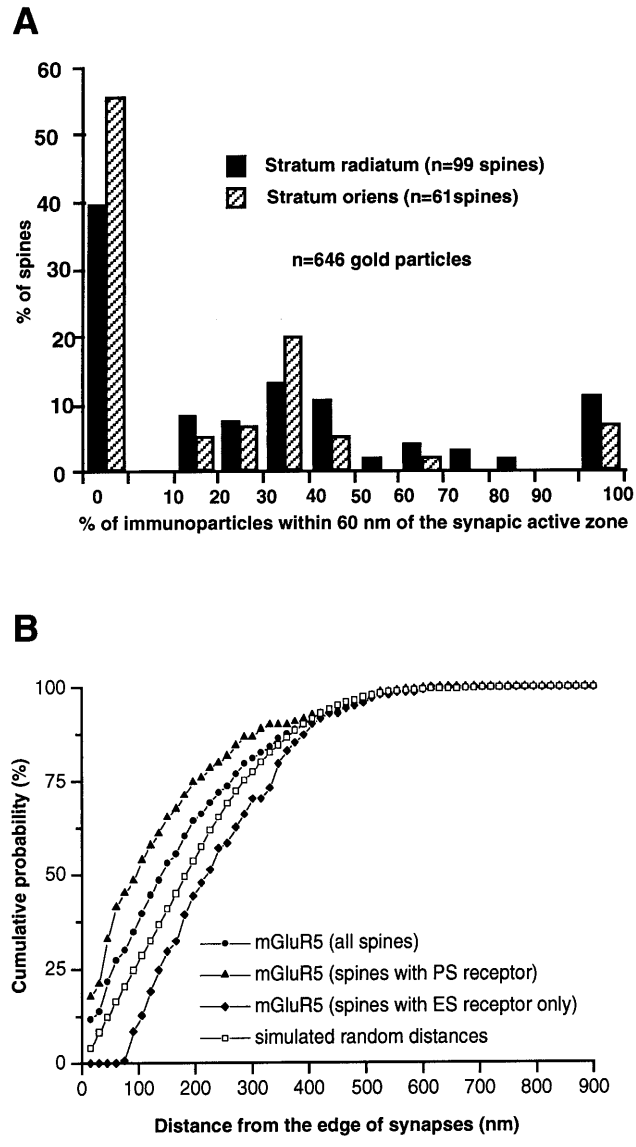

Fig. 7. Dendritic spines are heterogeneous with respect to the precise location of mGluR5 relative to the synaptic active zone in the hippocampal CA1 region. (A) Distribution of immunopositive dendritic spines according to the position of mGluR5. Spines containing completely reconstructed postsynaptic membrane specialisation were assessed from serial sections. Spines are grouped according to the proportion of immunoparticles within 60 nm of the synaptic active zone. Both strata oriens and radiatum contain a substantial proportion of spines without immunoparticles within the perisynaptic annulus surrounding the synaptic junction, although the mean number of particles in these spines was not different ($P > 0.1$) from that of spines having various proportions (10–90%) of perisynaptic receptors. (B) Comparison of the position of immunoparticles for mGluR5 (same spine populations as in A) with simulated random distribution (□) on the same membrane surface. The cumulative probability plots and statistical comparisons demonstrate that the position of mGluR5 significantly differ from random distribution in the total spine population (●), in the spines with perisynaptic (PS) receptors (▲) and in the spines having extrasynaptic (ES) receptor only (◆).

sectioned membranes are uniformly exposed to the same concentration of antibody on the surface of the section. The post-embedding method however has a lower sensitivity with some antibodies than the pre-embedding method. From the antibodies used in the present study, under post-embedding conditions, the antibodies to mGluR5 and the monoclonal antibody to mGluR2 provided only a weak signal whereas the guinea pig antibody to mGluR2 could not be used, therefore we used pre-embedding conditions for quantification. The comparison carried out for mGluR1α and the qualitatively similar results obtained for mGluR5 using either method (Lujan et al., 1996) indicate that, for the localisation of mGluRs, the pre-embedding technique is suitable as far as the location in the plasma membrane is concerned. The limitation of differential diffusion of antibodies into the tissue and neighbouring cellular elements cannot, however, be excluded. Therefore, the absence of immunolabelling in elements close to immunopositive ones cannot be interpreted as indicating the absence of receptor.

The resolution of the pre-embedding technique is lower than that of the postembedding method ($\sim$ 20 nm) because the immunoparticles tend to be larger (up to 50–70 nm) in the former. In theory, using the indirect immunocytochemical method, the 1.4 nm gold particle is about 15 nm from the epitope, but the increase in particle size due to silver intensification, the joining of particles at sites of high density and the possible distortion introduced by glutaraldehyde fixation may introduce variables that make the location of epitope less well defined using the pre-embedding technique. Therefore, we chose a bin width of 60 nm for displaying the measurements, but this does not necessarily mean that the annulus having high receptor density and surrounding the synaptic density is so wide; it could be much narrower.

The postsynaptic membrane specialisation has a fuzzy edge which is difficult to define precisely both in anatomical and in molecular terms. Both the pre- and the post-embedding immunocytochemical methods show the highest concentration of group I receptors at the edge of the postsynaptic specialisation, the particles often overlapping with the fuzzy edge of electron opaque material. The pool of receptor within 60 nm of the electron microscopically detectable edge of the fuzzy material is termed the 'perisynaptic' pool. At present, in the absence of co-labelling with markers exclusively present in the postsynaptic density, it is not possible to determine whether the particles apparently overlapping with the postsynaptic density are in the most peripheral part of the postsynaptic density or just adjacent to it. The main reason for this uncertainty is that the edge of the synapse can change substantially in tangential position within the 80 nm depth of the section which provides the image. In some cases the particles appear to overlap with the edge of the postsynaptic density; in others they appear to be just lateral to it. In any case, in terms of glutamate concentration and time course there would be no differences over such a short distance. However, as the postsynaptic density is clearly a distinct molecular environment, the receptor anchoring and transduction mechanisms may change abruptly at the edge of the postsynaptic density.

The comparison of the relative densities and the fraction of receptors in relation to synapses assumes that the signal is not saturated at sites of high receptor density. For mGluR2 this could well be the case, because it occurred at relatively low density. For mGluR5, a 25% labelling frequency (two sides of the synapse treated as independent occurrences) was observed at the site of highest density in the perisynaptic position of immunolabelled spines, as detected in individual section. Therefore, provided that the receptor is not grouped in the perisynaptic position, it is unlikely that the labelling is saturated. However, for mGluR1α, up to 50% of perisynaptic sites (two sides of the synapse treated as independent occurrences) were labelled in single sections, indicating a very high density of perisynaptic receptor. Therefore, the saturation of the signal cannot be excluded. If it occurred, the measurements would tend to underestimate the fraction of receptor at the edge of the synapse.

4.2. Compartmental location of mGluRs in the plasma membrane

As described earlier, in several areas of the central nervous system (Baude et al., 1993; Nusser et al., 1994; Vidnyanszky et al., 1994; Lujan et al., 1996; Vidnyanszky et al., 1996) mGluR1 and mGluR5 are located at both perisynaptic and extrasynaptic sites. Moreover, splice variant mGluR1α (Baude et al., 1993; Nusser et al., 1994) as well as mGluR1b/c (Lujan et al., 1996) show this pattern. The present quantification extends these findings and demonstrates that, taking into account several correction factors, the fraction of receptor in this perisynaptic pool is significantly different for the two receptor subtypes. Even comparing only those mGluR5 positive pyramidal spines which have a perisynaptic receptor pool with mGluR1α positive Purkinje cell spines, the receptor distributions are significantly different.

In our previous quantitative study of mGluR5 on dendritic spines there appeared to be three levels of receptor density in the membrane of hippocampal pyramidal cell spines as a function of distance from the edge of the synaptic specialisation (Lujan et al., 1996). However, in the previous calculation only the frequency of receptor labelling was recorded for each position which gave a measure of the relative densities of receptor at a given distance from the synapse. In the present calculation we have compared the fraction of receptors at a

given position and have taken into account the differences in spine membrane area as a function of distance from the synapse, approximating spine heads as spheres. Although in general there is agreement between the two representations, the latter calculation gives a better overall picture of the relative amount of receptor at any given distance from the synapse. Both calculations have the limitation that they cannot account for the differences in the shape, size and receptor content of individual spines. Nevertheless they proved to be useful for revealing differences between cell types and receptor subtypes.

Different positions on dendritic spines may represent differences in the location of isoforms mGluR5a and mGluR5b, both of which would be recognised by our antibodies. Although the extent of expression of the two isoforms changes during development (Minakami et al., 1995; Romano et al., 1996) both are expressed in the adult hippocampus. The mGluR5b protein contains an additional 32 amino acid sequence (Minakami et al., 1993), as compared with the mGluR5a, which could lead to differences in function and location of the receptor. For example, one splice variant may be preferentially located at the edge of the postsynaptic density. Unfortunately, the physiological significance of the isoform diversity of mGluR5 remains unknown (Joly et al., 1995). Since the insertion is in the C-terminal intracellular domain of the protein, it remains to be tested if the two isoforms can interact with other proteins in a differential manner.

The comparison of the distribution of mGluR5 with mGluR1α revealed that the latter is much more highly enriched immediately adjacent to the postsynaptic membrane specialisation. Using mean parameters of spines it has been calculated that, in relative terms, at least twice as high a fraction of spine mGluR1α is at the edge of the synaptic junction as mGluR5. The decline in receptor fraction as a function of distance from the synapse is monotonic for mGluR1α, suggesting a single effector mechanism, and is much steeper than for mGluR5.

The association of a large fraction of both mGluR1α and mGluR5 with the edge of the synaptic junction made by the terminal innervating a given dendritic spine, suggests input specificity for the activation of the perisynaptic pool of receptors. As the distance increases from the synapse the likelihood that the extrasynaptic receptor pools are exposed to transmitter released from other terminals increases, particularly in the hippocampus where the spines are not isolated from each other by glial lamellae as in the cerebellum. However, the fraction of the extrasynaptic receptor pool decreases due to the decline in receptor density as well as in the area of membrane towards the neck of the spine. The receptor density then remains at a low level throughout the somato-dendritic domain of Purkinje cells and CA1 pyramidal cells, but because the extrasynaptic membrane area of both cell types is much larger than the perisynaptic zone the overall fraction of receptor away from the synapses received by the cell is not insignificant.

The distribution of mGluR2 in the plasma membrane of Golgi cells does not reflect input specificity of activation. The transmitter activating mGluR2 could originate from synaptic terminals innervating the cell, from terminals innervating other cells, or from glial cells. Although the position of mGluR2 relative to parallel fibre terminals does not differ from random distribution, overall, mGluR2 is not randomly distributed in the membrane, but appears to occur in patches of higher receptor density interspersed by areas of scattered receptors at low density. It will be interesting to establish whether potential effector molecules are also distributed in patches in the somato-dendritic membrane.

The striking difference between the location of mGluR2 on Golgi cells and mGluR1α on Purkinje cells may provide a clue for an additional factor influencing receptor distribution. Both cells receive input from parallel fibre terminals, but the Purkinje cell spine is intimately surrounded by glial lamellae (see e.g. Somogyi et al., 1990), whereas the terminals on interneuron dendrites lack the glial wrapping. In an elegant quantitative, post-embedding immuno-localisation study Chaudhry et al. (1995) demonstrated that two glial glutamate transporters, GLAST and GLT, occurred at a much higher density around Purkinje cell spine synapses than around the synapses on interneuron dendrites (e.g. Golgi cells). Thus, due to the difference in binding to transporters the extrasynaptic spine membrane would be exposed to a lower and more steeply declining glutamate concentration than the interneuron dendritic membrane. The much tighter association of postsynaptic mGluR1α with the release site on spines, as compared to mGluR2 on dendritic shafts may reflect the fine tuning of receptor location to such a predicted difference in transmitter concentration. Of course, since many other differences exist between the two synapses and receptors, other factors are just as likely to make a contribution.

4.3. Are different effector mechanisms co-localised with distinct pools of mGluR on the same cell?

The pools of mGluR5 in the plasma membrane of dendritic spines and dendritic shafts of pyramidal cells, or mGluR5 having different position on the same dendritic spine, could be coupled to different effector mechanisms (reviewed by Gerber and Gahwiler, 1994; Pin and Duvoisin, 1995). Group I mGluRs regulate pyramidal cell activity by potentiating NMDA receptor-mediated responses (Aniksztejn et al., 1992; Fitzjohn et al., 1996), suppressing several types of potassium and calcium currents (Baskys et al., 1990; Charpak et al., 1990; Lester and Jahr, 1990; Gerber et al., 1992; Sahara and Westbrook, 1993) and activating a non-selective cationic

current (Crepel et al., 1994; Guerineau et al., 1994). The modulation of one of the potassium currents, IK_{AHP}, does not require the activation of the enzymes PKC, PKA or CaMKII (Gerber et al., 1992; Muller et al., 1992), but the potentiation of NMDA receptor-mediated responses in CA1 pyramidal cells involves the activation of PKC (Aniksztejn et al., 1992), although additional mechanisms not involving PKC may also be involved (Harvey and Collingridge, 1993). The precise location of the ion channels and the enzymes that mediate their modulation by mGluR5, the principal Group I mGluR in the somato-dendritic domain of CA1 pyramidal cells (Abe et al., 1992), is not known. One possibility is that they are diffusely distributed in the plasma membrane and the mGluR5-evoked rise in second messenger, such as Ca^{2+} released from intracellular stores, uniformly activates all mechanisms. However, CA1 pyramidal cells may be able to compartmentalise ion channels to distinct plasma membrane domains which would enhance their coupling to co-localised receptor pools, including mGluR5. In line with this suggestion, NMDA type glutamate receptors are likely to be concentrated in the postsynaptic density (Kharazia et al., 1996), making the perisynaptic mGluR5 pool at the edge of the synaptic junction the most likely candidate to regulate them. Many of the small dendritic spines that have mGluR5 do not appear to have smooth ER (Spacek and Harris, 1997) that serves as the IP3 sensitive Ca^{2+} store, therefore the high level mGluR5-containing zone of extrasynaptic membrane may be involved in the suppression of K^+ channels that do not require the involvement of Ca^{2+} (Charpak et al., 1990; Glaum and Miller, 1992). Finally, the postsynaptic mechanisms that involve the release of calcium, such as the activation of the non-specific cation current (Crepel et al., 1994, but see Guerineau et al., 1995 for CA3 cells) may be preferentially located furthest from the synapse in the zone of low mGluR density on spines, their necks and in the dendritic shaft membrane, which are closest to the Ca^{2+} store in the smooth ER. Of course, as suggested by the variation of mGluR5 position on individual spines (see below), different physiological states of single spines may result in dynamic changes in the distribution of the effector mechanisms as well.

In the cerebellum mGluR1 activation evokes an inward current and depolarisation of Purkinje cells, which is consistent with the activation of a calcium-dependent non-specific cation current (Staub et al., 1992; Batchelor and Garthwaite, 1997) or an electrogenic sodium/calcium exchanger (Glaum et al., 1992; Staub et al., 1992). The activation of mGluR1 is a necessary component of producing Ca^{2+}-dependent long-term depression of AMPA receptor-mediated synaptic responses of parallel fibre synapses (Shigemoto et al., 1994; reviewed by Linden and Connor, 1995). Immunocytochemical studies confirmed that AMPA type (Baude et al., 1993; Nusser et al., 1994) and delta (Landsend et al., 1997) glutamate receptors are concentrated in the synaptic specialisation. Since the pool of mGluR1α in spines is strongly and unimodally aligned to the parallel fibre synapses, it is possible that a single transduction and effector mechanism explains its role in the function of parallel fibre synapses. The location and relative densities of the other mGluR1 isoforms remain to be determined.

The effector mechanism of mGluR2 activation in Golgi cells is not known, and it may be different in the somato-dendritic and axonal domains. The activation of mGluR2 in a heterologous expression system produced strong inhibition of forskolin stimulated cAMP formation (Tanabe et al., 1992) and reduced Ca^{2+} influx into olfactory bulb interneurons (Bischofberger and Schild, 1996). Since the activation of group-II mGluRs and the suppression of cAMP production reduces transmitter release (for review see Pin and Duvoisin, 1995) it is likely that mGluR2 activation on Golgi cell terminals has a similar effect. Regarding the effect of mGluR2 activation on the somato-dendritic domain, it is noteworthy that an inhibitory action of glutamate on the firing of some neurons in the granule cell layer have been reported (Yamamoto et al., 1976). These cells may have been Golgi cells as suggested by the authors, and this would indicate that mGluR2 activation leads to postsynaptic inhibition, which might explain why the receptor is not localised near parallel fibre synapses activating Golgi cells.

4.4. Heterogeneity of dendritic spines in CA1 pyramidal cells

The quantitative comparison of individual dendritic spines revealed that nearly half of the immunopositive spines lacked mGluR5 in a perisynaptic position, whereas the remaining spines had a wide range of receptor fraction at the edge of the synaptic active zone. Such heterogeneity may correlate with the origin of presynaptic terminals. In the stratum oriens there are at least three sources of glutamatergic terminals making asymmetrical synapses: Schaffer collaterals from the CA3 area, local collaterals of the CA1 pyramidal cells and the alvear input from the entorhinal cortex (Deller et al., 1996; Sanz et al., 1996). Whether the differences in mGluR5 location are correlated with the source of input to the spine remains to be determined. However, the heterogeneity of inputs is unlikely to be an explanation in stratum radiatum, because although CA1 pyramidal axon collaterals and entorhinal synaptic inputs are present in stratum radiatum (Sanz et al., 1996), they represent a much smaller fraction of synapses than in stratum oriens and the heterogeneity of mGluR5 fractional distribution is the same in both layers.

A more likely reason for the distinct spine populations may be related to different physiological states. If the different locations along the spine membrane correspond

to different transduction and effector mechanisms, as suggested above, then it is possible that, depending on the state of a spine and its synaptic input, distinct roles of the receptor are represented with a different weight in a spine specific manner. For example, if the primary role of the perisynaptic pool associated with the edge of the synaptic specialisation was the modulation of synaptic NMDA receptors via PKC, then such an effector mechanism would be reduced in spines lacking the perisynaptic pool. The fraction of the different pools, however, may vary dynamically by the translocation of receptors. Cytoplasmic proteins associated with the intracellular domain of mGluR5 such as the protein 'homer' (Brakeman et al., 1997), which can be induced by increased synaptic activity, may play a role in the translocation of the receptor within the spine. Another consequence of the heterogeneity of mGluR5 distribution in spines is that the input specificity of mGluR activation is likely to be lower for spines which exclusively or mainly contain receptors away from the glutamatergic synapse.

4.5. Presynaptic location of mGluR2 in GABAergic Golgi cells

In previous electron microscopic studies, mGluR1α/b/c and mGluR5a/b were only found in the somatodendritic plasma membrane in the cerebellum and hippocampus (Martin et al., 1992; Baude et al., 1993; Shigemoto et al., 1993; Lujan et al., 1996). In contrast, mGluR2/3 was found at both postsynaptic and presynaptic domains in the same cell type, the Golgi cell (Ohishi et al., 1994; Neki et al., 1996a,b). The immunogold labelling revealed that, similar to the dendritic domain, mGluR2 does not seem to be associated with any particular area along the axons and terminals whether they made symmetrical or asymmetrical synapses, therefore it probably acts as a heteroreceptor. The pattern of mGluR2 in GABAergic terminals is also different from mGluR7, a member of receptor group III, which is predominantly located in the presynaptic membrane specialisation in glutamatergic terminals, and probably acts as an autoreceptor (Shigemoto et al., 1996). A surprisingly high fraction of immunoreactivity for mGluR2 was located within the terminal, associated with the smooth ER and predicting a high receptor turnover, which is also supported by the frequent labelling of the somatic rough ER.

Generally, Golgi cell terminals are at the periphery of the glomeruli, separated from the mossy fibre terminals which contain glutamate (Somogyi et al., 1986) by an interwoven meshwork of granule cell dendrites. It has been proposed that glutamate released from mossy fibre terminals may diffuse and reach Golgi cell terminals activating mGluR2 by a mechanism of transmitter spillover (Ohishi et al., 1994). Alternatively, glutamate or some other endogenous mGluR agonist may be released by granule cell dendrites and act in a retrograde manner on Golgi cell terminals, as suggested for interneuron to Purkinje cell GABAergic synapses (Glitsch et al., 1996).

4.6. Possible role of the C-terminal domain in the precise location of mGluRs

The mechanism of mGluR targeting and membrane anchoring is unknown, but the presence of multiple receptor pools in the plasma membrane suggests several mechanisms. Interestingly, the two group I mGluRs, which have a pool associated with the edge of synapses in Golgi cells, have a long C-terminal intracellular domain, with more than 350 residues, whereas the two group-II mGluRs, one of which as we have shown is not associated with synapses, have a shorter C-terminus, with only 48 residues. However, the difference in receptor subtype location cannot simply be a consequence of the length of the C-termini because mGluR1b/c which have short C-termini, were also found in perisynaptic position (Lujan et al., 1996). In cerebellar Purkinje cells, which express mRNA for the three mGluR1 splice variants (Pin et al., 1992), both mGluR1α and mGluR1b appear to be present in dendritic spines (Grandes et al., 1994). Whether the degree of their synaptic alignment is similar remains to be established. The two splice variants of mGluR5 which differ in a C-terminal insertion could also be related to differential location since so far no functional difference has been detected between them (see above).

It is possible that the C-terminal domain allows mGluR1α and mGluR5 to be expressed at a higher density at the edge of the synaptic junction by facilitating the coupling of the receptors to postsynaptic density molecules at the edge of the synapse. A soluble protein named 'homer', containing a PDZ domain has recently been cloned and shown to interact with the C-termini of group I mGluRs (Brakeman et al., 1997). Interaction of the C-terminal domain of the NR2B subunit of the NMDA receptor with several synapse associated proteins has been demonstrated (Kornau et al., 1995; Kim et al., 1996). Similarly, other glutamate receptor subunits, the GluR2 and GluR3 subunits of the AMPA type receptor, were also found to interact with a synapse associated protein (Dong et al., 1997). In addition to localising the receptors, the C-terminal domain may play other roles in the function of mGluRs, as mGluR1α has different functional characteristics from the shorter proteins mGluR1b and mGluR1c (Pickering et al., 1993; Pin et al., 1992; Joly et al., 1995). In contrast, no functional differences were observed when mGluR1α was compared with mGluR5a and b (Joly et al., 1995), all containing a long C-terminal domain of more than 350 amino acids. The C-terminus of

mGluRs, together with other intracellular domains, has been proposed to be involved in the coupling efficiency to G proteins (Gomeza et al., 1996; Prezeau et al., 1996). Moreover, changes in the C-terminal domain can generate receptors with different transduction mechanisms, as functional studies have demonstrated for the prostaglandin EP3 receptor (Namba et al., 1993; Sugimoto et al., 1993), a member of the seven transmembrane domain receptor family.

4.7. Possible functional consequence of graded group I mGluR distribution

In several physiological experiments, the activation of mGluRs by synaptically released transmitter could be detected only after activating the presynaptic input repeatedly (Charpak and Gahwiler, 1991; Miles and Poncer, 1993; Batchelor et al., 1994; Batchelor and Garthwaite, 1997). This indicates that detectable receptor activation in many cells requires repeated release of glutamate in order to reach sufficiently high levels at the extrasynaptic mGluR sites as suggested earlier (Baude et al., 1993; Nusser et al., 1994). In addition to the frequency of release, the extracellular concentration of glutamate also depends on the efficacy of neuronal and glial uptake, the number of receptors and transporters, the tortuosity of the extracellular space and other factors, all of which are likely to be specific and optimised for a given type of synaptic connection (for review see Clements, 1996). The density gradient differences in mGluR distribution, in a synapse and cell type specific manner, probably also reflect the optimisation of mGluR activation as a function of the amount of released glutamate. The degree of activation is probably non-linearly related to glutamate release frequency, partly due to the specific receptor density gradients demonstrated in this study. The possible differential location of distinct effector mechanisms activated by the same receptor subtype on the same cell could also introduce additional non-linearity into the transmitter release frequency-dependent effects of mGluRs.

Acknowledgements

The authors are grateful to Dr Tibor Szilagyi and Mr Laszlo Marton for advice, helpful discussions, providing the simulations of receptor distribution and the cylindrical approximation of dendritic surface (L.M.). The brain of a mGluR2 deficient mouse was kindly provided by Drs M. Yokoi and S. Nakanishi for testing of the specificity of one of the antibodies. The authors also thank Dr Jeff McIlhinney for critical comments and Dr Zoltan Nusser for help with the statistics, for helpful discussion during the project and for his comments on an earlier version of the manuscript. The technical assistance of Ms Zahida Ahmad and the photographic assistance of Mr Frank Kennedy, Mr Paul Jays and Mr Akira Uesugi are acknowledged. This work was partly supported by grants from the Japan Society for the Promotion of Science, the British Council and the Royal Society.

References

Abe, T., Sugihara, H., Nawa, H., Shigemoto, R., Mizuno, N., Nakanishi, S., 1992. Molecular characterization of a novel metabotropic glutamate receptor mGluR5 coupled to inositol phosphate/Ca^{2+} signal transduction. J. Biol. Chem. 267, 13361–13368.

Aniksztejn, L., Otani, S., Ben-Ari, Y., 1992. Quisqualate metabotropic receptors modulate NMDA currents and facilitate induction of long-term potentiation through protein kinase C. Eur. J. Neurosci. 4, 500–505.

Aramori, I., Nakanishi, S., 1992. Signal transduction and pharmacological characteristics of a metabotropic glutamate receptor, mGluR1, in transfected CHO cells. Neuron 8, 757–766.

Baskys, A., Bernstein, N.K., Barolet, A.W., Carlen, P.L., 1990. NMDA and quisqualate reduce a Ca-dependent K^+ current by a protein kinase-mediated mechanism. Neurosci. Lett. 112, 76–81.

Batchelor, A.M., Garthwaite, J., 1997. Frequency detection and temporally dispersed synaptic signal association through a metabotropic glutamate receptor pathway. Nature 385, 74–77.

Batchelor, A.M., Madge, D.J., Garthwaite, J., 1994. Synaptic activation of metabotropic glutamate receptors in the parallel fibre-Purkinje cell pathway in rat cerebellar slices. Neuroscience 63, 911–915.

Baude, A., Nusser, Z., Roberts, J.D.B., Mulvihill, E., McIlhinney, R.A.J., Somogyi, P., 1993. The metabotropic glutamate receptor (mGluR1α) is concentrated at perisynaptic membrane of neuronal subpopulations as detected by immunogold reaction. Neuron 11, 771–787.

Baude, A., Nusser, Z., Molnar, E., McIlhinney, R.A.J., Somogyi, P., 1995. High-resolution immunogold localization of AMPA type glutamate receptor subunits at synaptic and non-synaptic sites in rat hippocampus. Neuroscience 69, 1031–1055.

Beaulieu, C., Colonnier, M., 1983. The number of neurons in the different laminae of the binocular and monocular regions of area 17 in the cat. J. Comp. Neurol. 217, 337–344.

Bischofberger, J., Schild, D., 1996. Glutamate and *N*-acetylaspartylglutamate block HVA calcium currents in frog olfactory bulb interneurons via an mGluR2/3-like receptor. J. Neurophysiol. 76, 2089–2092.

Bradley, S.R., Levey, A.I., Hersch, S.M., Conn, P.J., 1996. Immunocytochemical localization of group III metabotropic glutamate receptors in the hippocampus with subtype-specific antibodies. J. Neurosci. 16, 2044–2056.

Brakeman, P.R., Lanahan, A.A., O'Brien, R., Roche, K., Barnes, C.A., Huganir, R.L., Worley, P.F., 1997. Homer: a protein that selectively binds metabotropic glutamate receptors. Nature 386, 284–288.

Brandstatter, J.H., Koulen, P., Kuhn, R., van der Putten, H., Wassle, H., 1996. Compartmental localization of a metabotropic glutamate receptor (mGluR7): two different active sites at a retinal synapse. J. Neurosci. 16, 4749–4756.

Charpak, S., Gahwiler, B.H., Do, K.Q., Knopfel, T., 1990. Potassium conductances in hippocampal neurons blocked by excitatory amino-acid transmitters. Nature 347, 765–767.

Charpak, S., Gahwiler, B.H., 1991. Glutamate mediates a slow synaptic response in hippocampal slice cultures. Proc. R. Soc. London Sci. 243, 221–226.

Chaudhry, F.A., Lehre, K.P., Campagne, M.V.L., Ottersen, O.P., Danbolt, N.C., Storm-Mathisen, J., 1995. Glutamate transporters in glial plasma membranes: highly differentiated localizations revealed by quantitative ultrastructural immunocytochemistry. Neuron 15, 711–720.

Clements, J.D., 1996. Transmitter timecourse in the synaptic cleft: its role in central synaptic function. Trends Neurosci. 19, 163–171.

Crepel, V., Aniksztejn, L., Ben-Ari, Y., Hammond, C., 1994. Glutamate metabotropic receptors increase a Ca^{2+}-activated nonspecific cationic current in CA1 hippocampal neurons. J. Neurophysiol. 72, 1561–1569.

Deller, T., Adelmann, G., Nitsch, R., Frotscher, M., 1996. The alvear pathway of the rat hippocampus. Cell Tissue Res. 286, 293–303.

Dong, H., OÕBrian, R.J., Fung, E.T., Lanahan, A.A., Worley, P.F., Huganir, R.L., 1997. GRIP: a synaptic PDZ domain-containing protein that interacts with AMPA receptors. Nature 386, 279–284.

Duvoisin, R.M., Zhang, C., Ramonell, K., 1995. A novel metabotropic glutamate receptor expressed in the retina and olfactory bulb. J. Neurosci. 15, 3075–3083.

Eaton, S.A., Birse, E.F., Wharton, B., Sunter, D.C., Udvarhelyi, P.M., Watkins, J.C., Salt, T.E., 1993. Mediation of thalamic sensory responses in vivo by ACPD-activated excitatory amino acid receptors. Eur. J. Neurosci. 5, 186–189.

Fitzjohn, S.M., Irving, A.J., Palmer, M.J., Harvey, J., Lodge, D., Collingridge, G.L., 1996. Activation of group I mGluRs potentiates NMDA responses in rat hippocampal slices. Neurosci. Lett. 203, 211–213.

Gerber, U., Sim, J.A., Gahwiler, B.H., 1992. Reduction of potassium conductances mediated by metabotropic glutamate receptors in rat CA3 pyramidal cells does not require protein kinase C or protein kinase A. Eur. J. Neurosci. 4, 792–797.

Gerber, U., Gahwiler, B.H., 1994. Modulation of ionic currents by metabotropic glutamate receptors in the CNS. In: Conn, P.J., Patel, J. (Eds.), The Metabotropic Glutamate Receptors. Humana Press, NJ, pp. 125–146.

Gereau, R.W., Conn, P.J., 1995. Roles of specific metabotropic glutamate receptor subtypes in regulation of hippocampal CA1 pyramidal cell excitability. J. Neurophysiol. 74, 122–129.

Glaum, S.R., Miller, R.J., 1992. Metabotropic glutamate receptors mediate excitatory transmission in the nucleus of the solitary tract. J. Neurosci. 12, 2251–2258.

Glaum, S.R., Slater, N.T., Rossi, D.J., Miller, R.J., 1992. Role of metabotropic glutamate (ACPD) receptors at the parallel fiber-Purkinje cell synapse. J. Neurophysiol. 68, 1453–1462.

Glitsch, M., Llano, I., Marty, A., 1996. Glutamate as a candidate retrograde messenger at interneurone-Purkinje cell synapses of rat cerebellum. J. Physiol. (London) 497, 531–537.

Gomeza, J., Joly, C., Kuhn, R., Knopfel, T., Bockaert, J., Pin, J.-P., 1996. The second intracellular loop of metabotropic glutamate receptor 1 cooperates with the other intracellular domains to control grouping to G-proteins. J. Biol. Chem. 271, 2199–2205.

Grandes, P., Mateos, J.M., Ruegg, D., Kuhn, R., Knopfel, T., 1994. Differential cellular localization of three splice variants of the mGluR1 metabotropic glutamate receptor in rat cerebellum. NeuroReport 5, 2249–2252.

Guerineau, N.C., Gahwiler, B.H., Gerber, U., 1994. Reduction of resting K^+ current by metabotropic glutamate and muscarinic receptors in rat CA3 cells: mediation by G-proteins. J. Physiol. 474, 27–33.

Guerineau, N.C., Bossu, J.-L., Gahwiler, B.H., Gerber, U., 1995. Activation of a nonselective cationic conductance by metabotropic glutamatergic and muscarinic agonists in CA3 pyramidal neurons of the rat hippocampus. J. Neurosci. 15, 4395–4407.

Harvey, J., Collingridge, G.L., 1993. Signal transduction pathways involved in the acute potentiation of NMDA responses by (1*S*,3*R*)-ACPD in rat hippocampal slices. Br. J. Pharmacol. 109, 1085–1090.

Hayashi, Y., Momiyama, A., Takahashi, T., Ohishi, H., Ogawa-Meguro, R., Shigemoto, R., Mizuno, N., Nakanishi, S., 1993. Role of a metabotropic glutamate receptor in synaptic modulation in the accessory olfactory bulb. Nature 366, 687–690.

Hollmann, M., Heinemann, S., 1994. Cloned glutamate receptors. Ann. Rev. Neurosci. 17, 31–108.

Joly, C., Gomeza, J., Brabet, I., Curry, K., Bockaert, J., Pin, J.-P., 1995. Molecular, functional and pharmacological characterization of the metabotropic glutamate receptor type 5 splice variants: comparison with mGluR1. J. Neurosci. 15, 3970–3981.

Kharazia, V.N., Phend, K.D., Rustioni, A., Weinberg, R.J., 1996. EM colocalization of AMPA and NMDA receptor subunits at synapses in rat cerebral cortex. Neurosci. Lett. 210, 37–40.

Kim, E., Cho, K.-O., Rothschild, A., Sheng, M., 1996. Heteromultimerization and NMDA receptor-clustering activity of chapsyn-110, a member of the PSD-95 family proteins. Neuron 17, 103–113.

Kinoshita, A., Ohishi, H., Neki, A., Nomura, S., Shigemoto, R., Takada, M., Nakanishi, S., Mizuno, N., 1996. Presynaptic localization of a metabotropic glutamate receptor, mGluR8, in the rhinencephalic areas: a light and electron microscope study in the rat. Neurosci. Lett. 207, 61–64.

Kornau, H.-C., Schenker, L.T., Kennedy, M.B., Seeburg, P.H., 1995. Domain interaction between NMDA receptor subunits and the postsynaptic density protein PSD-95. Science 269, 1737–1740.

Landsend, A.S., Amiry-Moghaddam, M., Matsubara, A., Bergersen, L., Usami, S., Wenthold, R.J., Ottersen, O.P., 1997. Differential localization of delta glutamate receptors in the rat cerebellum: Coexpression with AMPA receptors in parallel fiber-spine synapses and absence from climbing fiber-spine synapses. J. Neurosci. 17, 834–842.

Lester, R.A.J., Jahr, C.E., 1990. Quisqualate receptor-mediated depression of calcium currents in hippocampal neurons. Neuron 4, 741–749.

Linden, D.J., Connor, J.A., 1995. Long-term synaptic depression. Ann. Rev. Neurosci. 18, 319–357.

Lujan, R., Nusser, Z., Roberts, J.D.B., Shigemoto, R., Somogyi, P., 1996. Perisynaptic location of metabotropic glutamate receptors mGluR1 and mGluR5 on dendrites and dendritic spines in the rat hippocampus. Eur. J. Neurosci. 8, 1488–1500.

Martin, L.J., Blackstone, C.D., Huganir, R.L., Price, D.L., 1992. Cellular localization of a metabotropic glutamate receptor in rat brain. Neuron 9, 259–270.

Masu, M., Tanabe, Y., Tsuchida, K., Shigemoto, R., Nakanishi, S., 1991. Sequence and expression of a metabotropic glutamate receptor. Nature 349, 760–765.

Masu, M., Iwakabe, H., Tagawa, Y., Miyoshi, T., Yamashita, M., Fukuda, Y., Sasaki, H., Hiroi, K., Nakamura, Y., Shigemoto, R., Takada, M., Nakamura, K., Nakao, K., Katsuki, M., Nakanishi, S., 1995. Specific deficit of the ON response in visual transmission by targeted disruption of the mGluR6 gene. Cell 80, 757–765.

Matsubara, A., Laake, J.H., Davanger, S., Usami, S.I., Ottersen, O.P., 1996. Organization of AMPA receptor subunits at a glutamate synapse: a quantitative immunogold analysis of hair cell synapses in the rat organ of corti. J. Neurosci. 16, 4457–4467.

Miles, R., Poncer, J.-C., 1993. Metabotropic glutamate receptors mediate a post-tetanic excitation of guinea-pig hippocampal inhibitory neurones. J. Physiol. 463, 461–473.

Minakami, R., Katsuki, F., Sugiyama, H., 1993. A variant of metabotropic glutamate receptor subtype 5: an evolutionally conserved insertion with no termination codon. Biochem. Biophys. Res. Commun. 194, 622–627.

Minakami, R., Iida, K.-I., Hirakawa, N., Sugiyama, H., 1995. The expression of two splice variants of metabotropic glutamate receptor subtype 5 in the rat brain and neuronal cells during development. J. Neurochem. 65, 1536–1542.

Muller, D., Arai, A., Lynch, G., 1992. Factors governing the potentiation of NMDA receptor-mediated responses in hippocampus. Hippocampus 2, 29–38.

Naito, S., Ueda, T., 1981. Affinity-purified anti-protein I antibody. J. Biol. Chem. 256, 10657–10663.

Nakajima, Y., Iwakabe, H., Akazawa, C., Nawa, H., Shigemoto, R., Mizuno, N., Nakanishi, S., 1993. Molecular characterization of a novel retinal metabotropic glutamate receptor mGluR6 with a high agonist selectivity for L-2-amino-4-phosphonobutyrate. J. Biol. Chem. 268, 11868–11873.

Nakanishi, S., 1994. Metabotropic glutamate receptors: synaptic transmission, modulation, and plasticity. Neuron 13, 1031–1037.

Namba, T., Sugimoto, Y., Negishi, M., Irie, A., Ushikubi, F., Kakizuka, A., Ito, S., Ichikawa, A., Narumiya, S., 1993. Alternative splicing of C-terminal tail of prostaglandin E receptor subtype EP3 determines G-protein specificity. Nature 365, 166–170.

Neki, A., Ohishi, H., Kaneko, T., Shigemoto, R., Nakanishi, S., Mizuno, N., 1996a. Metabotropic glutamate receptors mGluR2 and mGluR5 are expressed in two non-overlapping populations of Golgi cells in the rat cerebellum. Neuroscience 75, 815–826.

Neki, A., Ohishi, N., Kaneko, T., Shigemoto, R., Nakanishi, S., Mizuno, N., 1996b. Pre- and postsynaptic localization of a metabotropic glutamate receptor, mGluR2, in the rat brain: an immunohistochemical study with a monoclonal antibody. Neurosci. Lett. 202, 197–200.

Nusser, Z., Mulvihill, E., Streit, P., Somogyi, P., 1994. Subsynaptic segregation of metabotropic and ionotropic glutamate receptors as revealed by immunogold localisation. Neuroscience 61, 421–427.

Nusser, Z., Roberts, J.D.B., Baude, A., Richards, J.G., Somogyi, P., 1995. Relative densities of synaptic and extrasynaptic $GABA_A$ receptors on cerebellar granule cells as determined by a quantitative immunogold method. J. Neurosci. 15, 2948–2960.

Ohishi, H., Shigemoto, R., Nakanishi, S., Mizuno, N., 1993a. Distribution of the messenger RNA for a metabotropic glutamate receptor, mGluR2, in the central nervous system of the rat. Neuroscience 53, 1009–1018.

Ohishi, H., Shigemoto, R., Nakanishi, S., Mizuno, N., 1993b. Distribution of the mRNA for a metabotropic glutamate receptor (mGluR3) in the rat brain: an in situ hybridization study. J. Comp. Neurol. 335, 252–266.

Ohishi, H., Ogawa-Meguro, R., Shigemoto, R., Kaneko, T., Nakanishi, S., Mizuno, N., 1994. Immunohistochemical localization of metabotropic glutamate receptors, mGluR2 and mGluR3, in rat cerebellar cortex. Neuron 13, 55–66.

Ohishi, H., Nomura, S., Ding, Y.-Q., Shigemoto, R., Wada, E., Kinoshita, A., Li, J.-L., Neki, A., Nakanishi, S., Mizuno, N., 1995. Presynaptic localization of a metabotropic glutamate receptor, mGluR7, in the primary afferent neurons: an immunohistochemical study in the rat. Neurosci. Lett. 202, 85–88.

Okamoto, N., Hori, S., Akazawa, C., Hayashi, Y., Shigemoto, R., Mizuno, N., Nakanishi, S., 1994. Molecular characterization of a new metabotropic glutamate receptor mGluR7 coupled to inhibitory cyclic AMP signal transduction. J. Biol. Chem. 269, 1231–1236.

Peters, A., Palay, S.L., Webster, H., 1991. The Fine Structure of the Nervous System. Oxford University Press, NY.

Petralia, R.S., Wang, Y.- X, Niedzielski, A.S., Wenthold, R.J., 1996. The metabotropic glutamate receptors, mGluR2 and mGluR3, show unique postsynaptic, presynaptic and glial localizations. Neuroscience 71, 949–976.

Pickering, D.S., Thomsen, C., Suzdak, P.D., Fletcher, E.J., Robitaille, R., Salter, M.W., MacDonald, J.F., Huang, X.-P., Hampson, D.R., 1993. A comparison of two alternatively spliced forms of a metabotropic glutamate receptor coupled to phosphoinositide turnover. J. Neurochem. 6, 85–92.

Pin, J.-P., Waeber, C., Prezeau, L., Bockaert, J., Heinemann, S.F., 1992. Alternative splicing generates metabotropic glutamate receptors inducing different patterns of calcium release in *Xenopus* oocytes. Proc. Natl. Acad. Sci. USA 89, 10331–10335.

Pin, J.-P., Duvoisin, R., 1995. Neurotransmitter receptors I. The metabotropic glutamate receptors: structure and functions. Neuropharmacology 34, 1–26.

Poncer, J.-C., Shinozaki, H., Miles, R., 1995. Dual modulation of synaptic inhibition by distinct metabotropic glutamate receptors in the rat hippocampus. J. Physiol. (London) 485, 121–134.

Prezeau, L., Gomeza, J., Ahern, S., Mary, S., Galvez, T., Bockaert, J., Pin, J.-P., 1996. Changes in the carboxyl-terminal domain of metabotropic glutamate receptor 1 by alternative splicing generate receptors with differing agonist-independent activity. Mol. Pharm. 49, 422–429.

Romano, C., Sesma, M.A., McDonald, C.T., O'Malley, K., van den Pol, A.N., Olney, J.W., 1995. Distribution of metabotropic glutamate receptor mGluR5 immunoreactivity in rat brain. J. Comp. Neurol. 355, 455–469.

Romano, C., van den Pol, A.N., O'Malley, K.L., 1996. Enhanced early developmental expression of the metabotropic glutamate receptor mGluR5 in rat brain: protein, mRNA splice variants and regional distribution. J. Comp. Neurol. 367, 403–412.

Sahara, Y., Westbrook, G.L., 1993. Modulation of calcium currents by a metabotropic glutamate receptor involves fast and slow kinetic components in cultured hippocampal neurons. J. Neurosci. 13, 3041–3050.

Sanchez-Prieto, J., Budd, D.C., Herrero, I., Vazquez, E., Nicholls, D.G., 1996. Presynaptic receptors and the control of glutamate exocytosis. Trends Neurosci. 19, 235–239.

Sanz, J.T., Shigemoto, R., Somogyi, P., 1996. Targeting of interneurons by entorhinal axons in stratum oriens and radiatum of area CA1 in the rat hippocampus. Brain Res. Assoc. Abstr. 13, 86.

Schoepp, D.D., Johnson, B.G., Salhoff, C.R., Valli, M.J., Desai, M.A., Burnett, J.P., Mayne, N.G., Monn, J.A., 1995. Selective inhibition of forskolin-stimulated cyclic AMP formation in rat hippocampus by a novel mGluR agonist, 2*R*,4*R*-4-aminopyrrolidine-2,4-dicarboxylate. Neuropharmacology 34, 843–850.

Seeburg, P.H., 1993. The TINS/TIPS lecture—the molecular biology of mammalian glutamate receptor channels. Trends Neurosci. 16, 359–365.

Shigemoto, R., Nomura, S., Ohishi, H., Sugihara, H., Nakanishi, S., Mizuno, N., 1993. Immunohistochemical localization of a metabotropic glutamate receptor, mGluR5, in the rat brain. Neurosci. Lett. 163, 53–57.

Shigemoto, R., Abe, T., Nomura, S., Nakanishi, S., Hirano, T., 1994. Antibodies inactivating mGluR1 metabotropic glutamate receptor block long-term depression in cultured Purkinje cells. Neuron 12, 1245–1255.

Shigemoto, R., Wada, E., Ohishi, H., Takada, M., Mizuno, N., Roberts, J.D.B., Somogyi, P., 1995. Differential presynaptic localization of metabotropic glutamate receptor subtypes, mGluR2/3 and mGluR7, in the rat hippocampus. Soc. Neurosci. Abstr. 21, 846.

Shigemoto, R., Kulik, A., Roberts, J.D.B., Ohishi, H., Nusser, Z., Kaneko, T., Somogyi, P., 1996. Target-cell-specific concentration of a metabotropic glutamate receptor in the presynaptic active zone. Nature 381, 523–525.

Somogyi, P., Halasy, K., Somogyi, J., Storm-Mathisen, J., Ottersen, O.P., 1986. Quantification of immunogold labelling reveals enrichment of glutamate in mossy and parallel fibre terminals in cat cerebellum. Neuroscience 19, 1045–1050.

Somogyi, P., Eshhar, N., Teichberg, V.I., Roberts, J.D.B., 1990. Subcellular localization of a putative kainate receptor in Bergmann Glial cells using a monoclonal antibody in the chick and fish cerebellar cortex. Neuroscience 35, 9–30.

Spacek, J., Harris, K.M., 1997. Three-dimensional organization of smooth endoplasmic reticulum in hippocampal CA1 dendrites and

dendritic spines of the immature and mature rat. J. Neurosci. 17, 190–203.

Staub, C., Vranesic, I., Knopfel, T., 1992. Responses to metabotropic glutamate receptor activation in cerebellar Purkinje cells: induction of an inward current. Eur. J. Neurosci. 4, 832–839.

Sugimoto, Y., Negishi, M., Hayashi, Y., Namba, T., Honda, A., Watabe, A., Hirata, M., Narumiya, S., Ichikawa, A., 1993. Two isoforms of the EP3 receptor with different carboxyl-terminal domains. Identical ligand binding properties and different coupling properties with Gi proteins. J. Biol. Chem. 268, 2712–2718.

Tanabe, Y., Masu, M., Ishii, T., Shigemoto, R., Nakanishi, S., 1992. A family of metabotropic glutamate receptors. Neuron 8, 169–180.

Tanabe, Y., Nomura, A., Masu, M., Shigemoto, R., Mizuno, N., Nakanishi, S., 1993. Signal transduction, pharmacological properties, and expression patterns of two rat metabotropic glutamate receptors, mGluR3 and mGluR4. J. Neurosci. 13, 1372–1378.

van den Pol, A.N., 1994. Metabotropic glutamate receptor mGluR1 distribution and ultrastructural localization in hypothalamus. J. Comp. Neurol. 349, 615–632.

van den Pol, A.N., Romano, C., Ghosh, P., 1995. Metabotropic glutamate receptor mGluR5 subcellular distribution and developmental expression in hypothalamus. J. Comp. Neurol. 362, 134–150.

Vidnyanszky, Z., Hamori, J., Negyessy, L., Ruegg, D., Knopfel, T., Kuhn, R., Gorcs, T.J., 1994. Cellular and subcellular localization of the mGluR5a metabotropic glutamate receptor in rat spinal cord. NeuroReport 6, 209–213.

Vidnyanszky, Z., Gorcs, T.J., Negyessy, L., Borostyankoi, Z., Kuhn, R., Knopfel, T., Hamori, J., 1996. Immunocytochemical visualization of the mGluR1α metabotropic glutamate receptor at synapses of corticothalamic terminals originating from area 17 of the rat. Eur. J. Neurosci. 8, 1061–1071.

Winsky, L., Nakata, H., Martin, B.M., Jacobowitz, D.M., 1989. Isolation, partial amino acid sequence, and immunohistochemical localization of a brain-specific calcium-binding protein. Proc. Natl. Acad. Sci. USA 86, 10139–10143.

Yamamoto, C., Yamashita, H., Chujo, T., 1976. Inhibitory action of glutamic acid on cerebellar interneurones. Nature 262, 786–787.

Yokoi, M., Kobayashi, K., Manabe, T., Takahashi, T., Sakaguchi, I., Katsuura, G., Shigemoto, R., Ohishi, H., Nomura, S., Nakamura, K., Nakao, K., Katsuki, M., Nakanishi, S., 1996. Impairment of hippocampal mossy fiber LTD in mice lacking mGluR2. Science 273, 645–647.